



Expertise
and insight
for the future

Sauli Sälemaa

Improvement of a Friction Test Machine

Metropolia University of Applied Sciences

Bachelor of Engineering

Mechanical and Production Engineering

Bachelor's Thesis

11 November 2019

Author Title	Sauli Sälemaa Improvement of a Friction Test Machine
Number of Pages Date	35 pages + 5 appendices 11 November 2019
Degree	Bachelor of Engineering
Degree Programme	Mechanical and Production Engineering
Professional Major	Machine Design
Instructors	Tuomas Teräsvuori, Project Manager Jyrki Kullaa, Principal Lecturer
<p>This thesis deals with the improvement of a friction test machine which has been designed by Rejlers Finland Oy. The machine has been built and during its testing, lack of compliance between the drives and the mechanisms, as well as the cumulative deflection caused by the lack of rigidity have caused the machine to be redesigned. The screw jack system was not compliant with the PID controller because the screw jack is irreversible, i.e. after the actuation force has been removed, the forces will not return without actuation to the original state. In consequence, the PID controller could not control the current of the servomotor, thus causing excessive forces during its operation and caused the rotary specimen to cut the plane.</p> <p>The primary objective of the thesis was to modify the screw jack system to be compliant with the internal PID controller. The secondary objective was to redesign the construction of the linear actuator carriage, and make it as stiff as possible within the constraints set by the original design.</p> <p>The designing of the assembly was carried out with SolidWorks 2018 software where the first friction test machine was already designed in CAD. The simulations were performed first with SolidWorks Simulation software, but after significant time consumption between the iterations, the simulations were conducted with Ansys Mechanical widely used in the mechanical finite element analysis.</p> <p>The modifications to the actuator mechanism assumed to be compliant with the PID controller. The simulations' results compared to the original design, had significant improvements in the stiffness of the system, without compromising the structural integrity or fatigue life of the machine. The project will be continued by the commissioning of the friction test machine prior to the delivery to the clients.</p>	
Keywords	mechanical design, stiffness improvements, SOLIDWORKS, FEA, ANSYS

Contents

List of Abbreviations

1	Introduction	1
1.1	Scope	1
1.2	Objective	3
2	Design	5
2.1	Engineering Constraints	5
2.2	Concepts	7
2.3	Modelling	9
3	Simulation	20
3.1	FEM Boundary Conditions	20
3.2	FEA Simulations and Results	20
4	Manufacturing	31
5	Conclusion	33
	References	35

Appendices

Appendix 1. HBM Force Transducer Data Sheet

Appendix 2. Hiwin RGW45CC Linear Guideway Specifications

Appendix 3. Hiwin Linear Guideways Mounting Positions

Appendix 4. The Dowel Pin Calculations

Appendix 5. Drawings

List of Abbreviations

AIT	Assembly, Integration and Test. Facility where assembly, integration and test can be done prior to commissioning the product to customer use.
CAD	Computer Aided Design. Software used designing and modelling 3D-models and assemblies.
FEA	Finite Element Analysis. Simulating a phenomenon with Finite Element Method.
FEM	Finite Element Method. A numerical method for solving problems of mathematical and engineering physics.
PID	Proportional–Integral–Derivative. Controller functioning on a control loop mechanism adjusted by feedback.

1 Introduction

This thesis was commissioned by Rejlers Finland Oy. Rejlers Group has over 2400 employees in over 80 locations in Finland, Sweden, Norway and Abu Dhabi. Rejlers Finland Oy is part of the Nordic based Rejlers group. Rejlers offers a variety of engineering and IT solutions for industrial, energy, construction, infrastructure and telecom areas. Rejlers Finland Oy has over 1000 employees in over 20 locations in Finland and one location in Abu Dhabi. In 2018 Rejlers Finland Oy had a turnover of a 56.2 million euros.

1.1 Scope

The thesis examines an existing friction test machine, which is a tailor made machine for Rejlers' clients. The goal of the machine is to measure static and dynamic friction coefficients by pressing a rotating cylindrical specimen on a flat motorized surface. The servo motor on the bottom frame plate rotates a screw jack system's worm screw that rotates the ball screw on top of the screw jack system. Thanks to the screw jack system, the linear actuator carriage moves up and down parallel to the linear guideway rails. The linear actuator carriage transmits force to the support on which the plane is mounted. The plane is pressed against a rotary specimen and both the force generated by the linear actuator carriage and the cradle torque are measured by force transducers. The data from the machine consists of the static and dynamic friction coefficients, which can be computed from the measured rotational torque, and the overall pressing force.

The scope of the thesis is limited to the linear force motorization of the flat surface, which will press against the cylindrical rotating specimen. It starts from the selection of the correct screw jack system, which in the existing machine, was a trapezoidal screw, which is irreversible. It is not compliant with the PID control loop system to which the servomotor has been designed for. The screw jack system is self-locking and the PID control cannot adjust the pressing force in real time as the PID controller controls the amperage of the servomotor. As the screw jack system is actuated up to a specified pressing force, when this specified force is achieved, the mechanism figuratively speaking locks itself, and no torque is transmitted back to the servomotor, and the controller cannot adjust the current, since no resistance is caused by the irreversibility of the system. This, in addition

to the force caused by the rotation of the cylindrical specimen, causes the system, more specifically the linear mechanism, to deform elastically, causing an increase in the linear force, which raised the overall force to very high forces. The servomotor should then decrease the force by winding the screw down, but due to the lack of feedback from the cumulative applied forces, the current at the servomotor cannot be adjusted. Furthermore, the force transducer stiffness is unknown, and therefore considered as negligible in the original design, which constituted a major factor in the overall deflection of the system.

As part of the scope, the overall number of linear bearing blocks and the mounting of the linear bearing blocks have to be revised, so that the mounting of the linear bearing blocks are as stiff as possible. In addition, the support holding the plane have to be aligned and rigidly connected to the linear actuator carriage to avoid the deflection as much as possible.

1.2 Objective

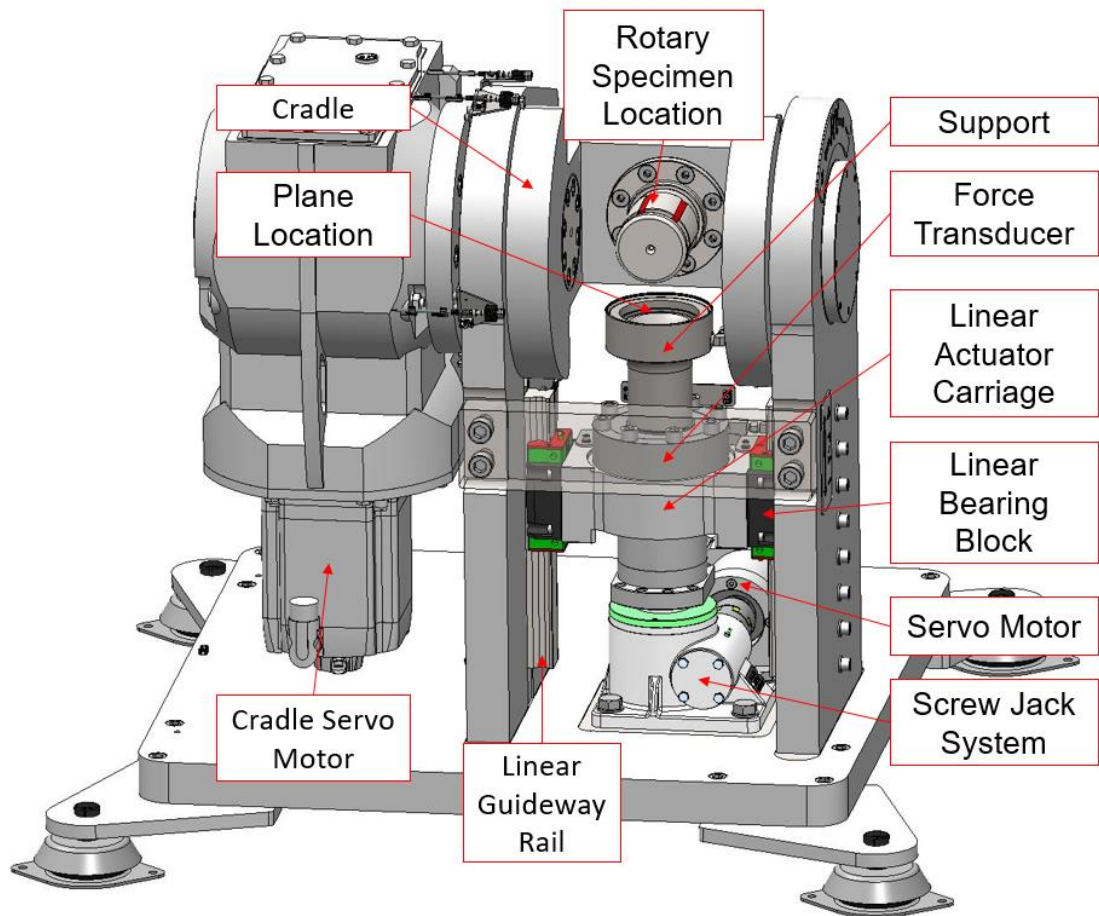


Figure 1. The friction test machine

The current screw system is shown in Figure 1, which is a significant constraint in the thesis, since the solution has been frozen at early stages in the design of the friction test machine. The friction test machine has been built and during its testing, cumulative deflection, due to lack of rigidity has been found, and therefore, the plane starts cutting into the rotary specimen with a large force.

The target is to find a solution which would require the minimum number of changes to the structures and fulfills the requirements for the PID loop, taking into account the hysteresis between rising and lowering the pressing force of the test plane. In addition, the linear actuator carriage and the support are to be designed again to make the friction test machine as stiff as possible. The deflection of the linear actuator carriage and the

support causes hysteresis of the system and can be seen as the “rolling” effect of the rotational test specimen on the plane, which causes a deviation in the direction of the loading, cumulating to issues with stiffness and measurement uncertainty.

All the improvements to design the new revision of the friction test machine are to be considered with FFF-fundamentals; Form, Fit and Function. Form takes into account the shape, dimensions, size, mass, material and other aesthetic choices, which produce the attractive aspect of the products. Fit will ensure that the designed components are able to interface physically with other parts, thus performing the new parts assemble straightforward. Function is the third and not the least issue which takes into consideration the actions the parts are designed to perform.

Table 1. Applicable standards

Ref.	Description	Document Number	Issue/Revision
AS1	Eurocode 3: General rules - Supplementary rules for cold-formed members and sheeting.	EN 1993-1-3	NA
AS2	Eurocode 3: Design of joints.	EN 1993-1-8	NA
AS3	Eurocode 3: Fatigue	EN 1993-1-9	NA

The mounting and quantity of the linear bearing blocks have to be enhanced. This can be done by tightening the linear bearing blocks using screws, which need to be calculated with regard to the preload forces, and the cutting forces present. It is important that the nominal slip force is at least 1.25 times the overall cutting force, as well as the nominal gapping force is to be 1.25 times the opening forces during normal conditions. These requirements are found in AS2 (see Table 1). The new mechanical design is to be calculated in static and elastic simulations, either with SolidWorks Simulation or with Ansys, which is available at the time needed.

The focus of the thesis is to produce a practical friction test machine by modifying the screw jack system to work with the PID controller and to increase the stiffness of the linear actuator carriage.

2 Design

2.1 Engineering Constraints

Constraints as mentioned above are the screw system, the force transducer, pressure test system and the frame, which have already been designed, purchased and manufactured and are not preferred to change. The space is considerably limited and have to be taken into account from the beginning. The first version of the friction test machine layout can be seen in Figure 2.

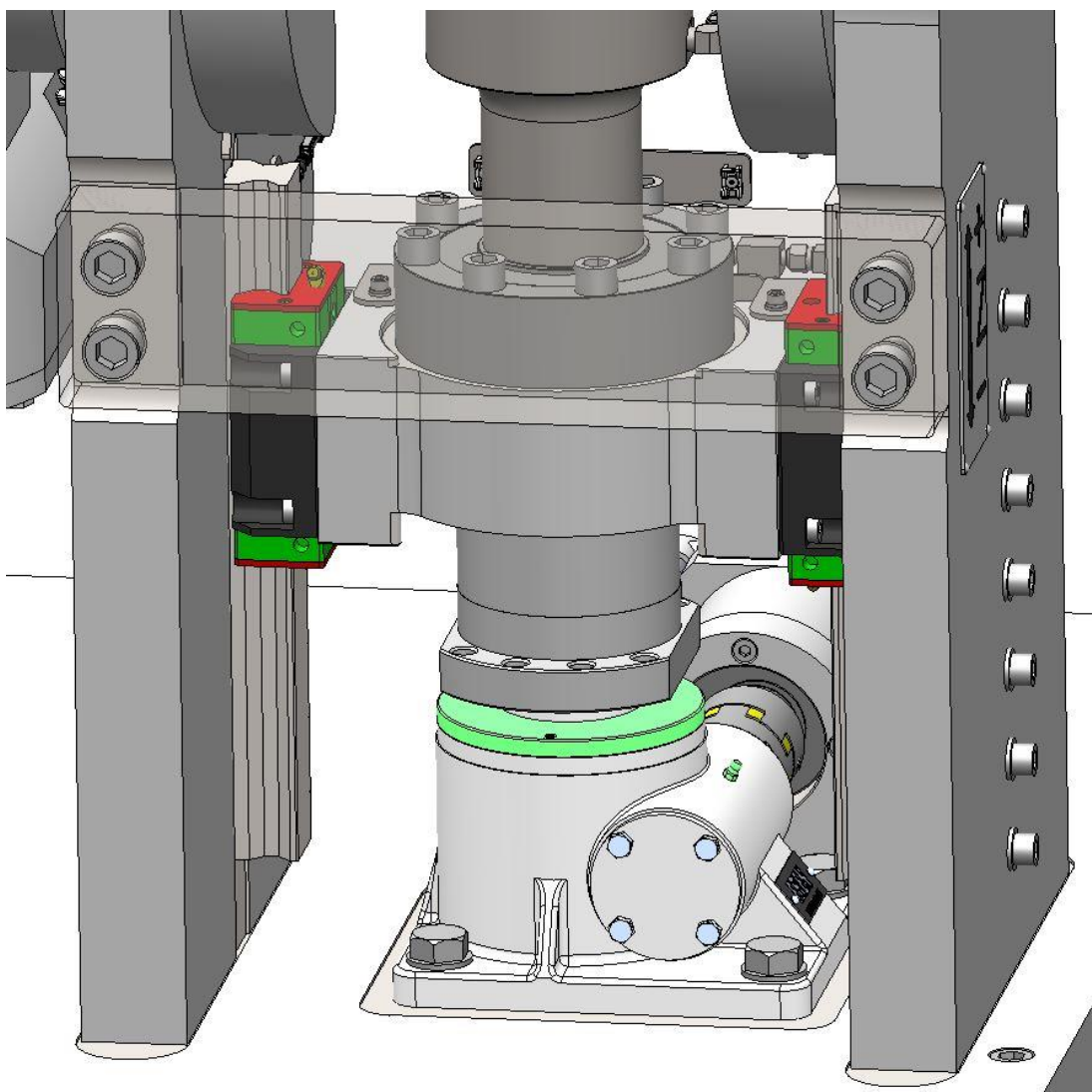


Figure 2. Order from top to bottom: the support, the force transducer, the linear actuator carriage and the screw jack system

The force transducers should not be changed, yet it is highly recommended to change the position to give the transducer a better lifespan, and by changing its position, is foreseen to improve the stiffness of the system. The required documentation of the transducer is found in Appendix 1. It is not obvious that by changing the position, the preload will be higher, which will need to be corrected by the software in the form of zeroing, or calibrating the transducer prior to the testing and commissioning of the friction test machine.

The current solution has on the rear side some pressure test equipment, which are attached to the main frame with two (2) bolted connections. These have to remain in that position, and are considered as constraints.

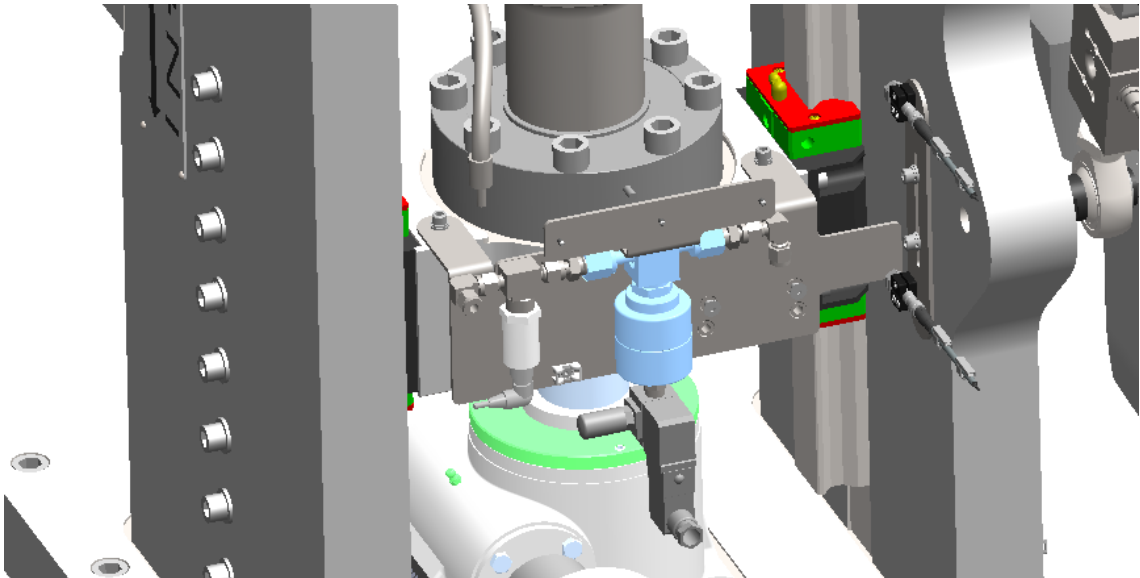


Figure 3. Pressure control equipment on the rear of the machine.

The snowball effect of such a structure being moved will cause possible changes in tubing, the location of energy chains, which are not foreseen to be necessary for the retrofitting. The pressure control valves are illustrated in Figure 3.

2.2 Concepts

Firstly, it was decided that the manufacturer would modify the screw system, to accompany the challenges of the PID control. The screw jack was changed to a reversible ball screw with a 12 mm pitch. In addition, the angle gear with worm gears inside the screw jack housing are replaced with gears that have a significantly higher pitch angle, making the system reversible. The initial casing retaining primary specifications to other components was used. After the changes made by the manufacturer, the screw jack system with a worm gear was tested prior to the delivery from FREN in Austria, in order to reduce possible risks of returning the screw for the second time, since the schedule for the modifications was tight. As a result, a load of 50 N on the screw body will cause a 0.015 Nm torque at the input shaft.

Secondly, the designing continued with sketching possible variations of the linear actuator carriage. Eliminating deflection in the y-direction as much as possible, the force transducer had to be moved lower. The screw system is so tall that it was not possible to set the sensor between the linear actuator carriage and the screw system, and for this reason it was positioned under the screw system. The linear actuator carriage was supported with two (2) Hiwin linear bearing blocks, which had one rail per each linear bearing block.

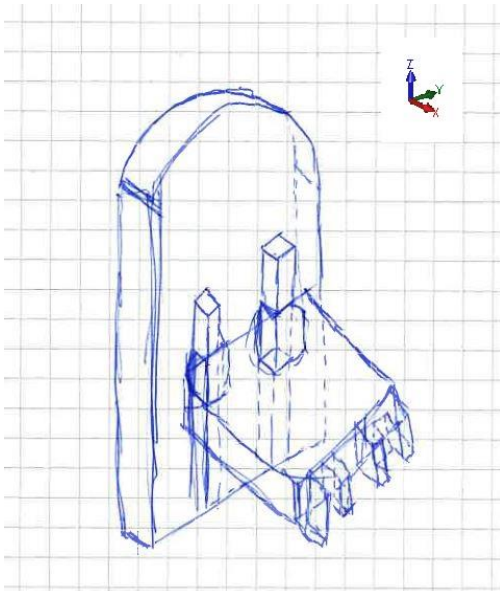


Figure 4. Sketch of linear guideways in XY-plane

One possible attachment of the linear actuator carriage was to place four (4) linear guideways in a rectangle at the XY-plane (Figure 4). Stiffness would have been substantially increased over the primary design, however the idea was then discarded because it would have required a major modification of the side plates of the frame where the rails attach.

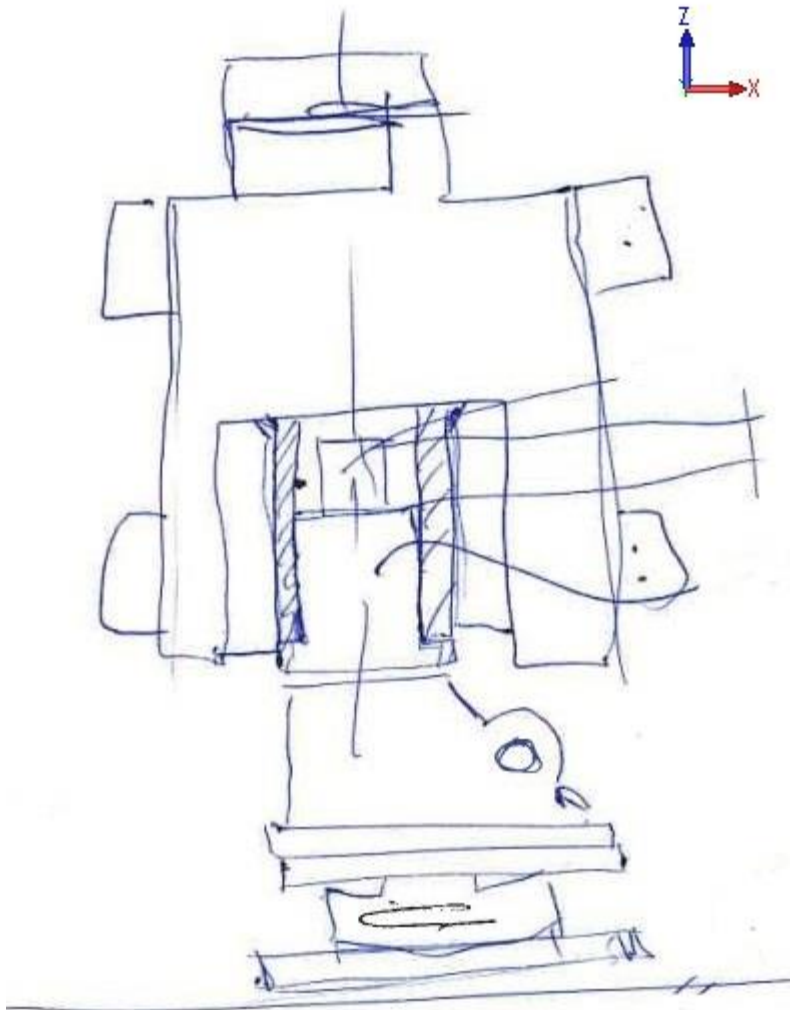


Figure 5. Sketch with linear bearing blocks in XZ-plane

Finally, the best option was to use the rails in the location where they were already positioned and place the four linear bearing blocks in the XZ-plane (Figure 5). This was the solution, which then was chosen and continued.

2.3 Modelling

Modelling was carried out using SolidWorks 2018 CAD (Computer Aided Design) software. The initial model has been modelled completely (Figure 6) in the above-mentioned software and therefore, it was proficient for modelling in CAD. As a result, the constraints for the FFF methods and requirements could be accomplished.



Figure 6. Main Assembly in CAD-software

Firstly, the force transducer was placed on the bottom frame with a plate to attach it to the already made holes on the bottom frame plate, where the screw system was previously attached. Therefore, drilling new holes to attach the force transducer would not have been required.

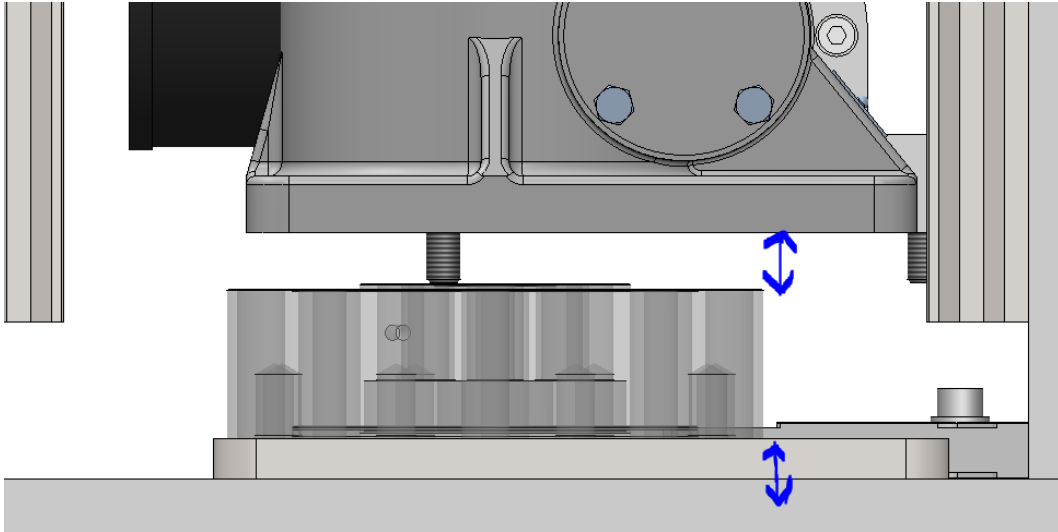


Figure 7. The force transducer with the attachment plate under

This made the space between the frame bottom plate and cradle even minor (see Figure 7). The decision was made that new holes would be made to the bottom frame plate and attach the force transducer directly to the bottom frame plate.

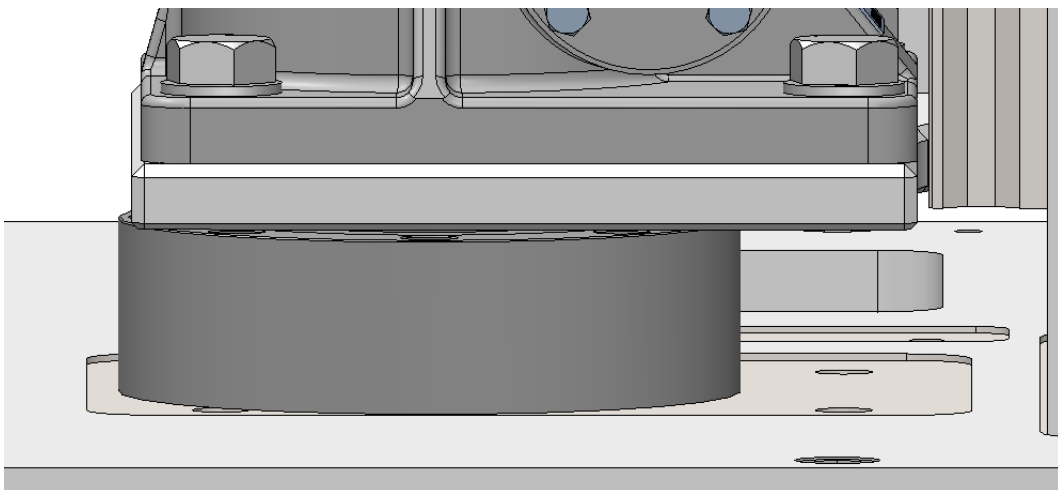


Figure 8. The force transducer attached to the bottom frame plate

This allowed 20 mm more space for the screw jack system and the linear actuator carriage (see Figure 8). In addition, it made possible the assembling of the force transducer and screw jack system together before assembling them to the main frame.

Secondly, the modified screw jack system was placed on top of the force transducer with an attachment plate to attach the screw system to the sensor. The plate was chosen to be a mould plate from Fodesco Oy because they provide plates with tight geometrical tolerances, which are more important than the dimensional tolerances, as seen in Figure 9.

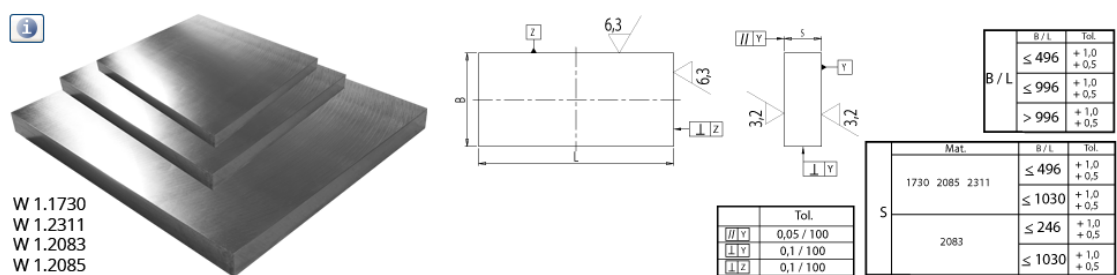


Figure 9. Fodesco milled blanks [2]

Fodesco Oy offered the machining of the plate to final measurements with rapid delivery time. The size of the plate is 346 x 296 mm and it was chosen from their catalog. It is a P - Standard plate for the production of plastic moulds. The size was chosen so that only one side and bottom required machining. The plate material was chosen to be DIN 1.2085 as it has excellent corrosion resistance with high yield strength, hardness and content of chrome. Steel's qualities in obtaining accurate tolerances and positive workability are better for this application. Furthermore, no coating is needed and the screw jack system and the force transducer can be assembled together in straight alignment.

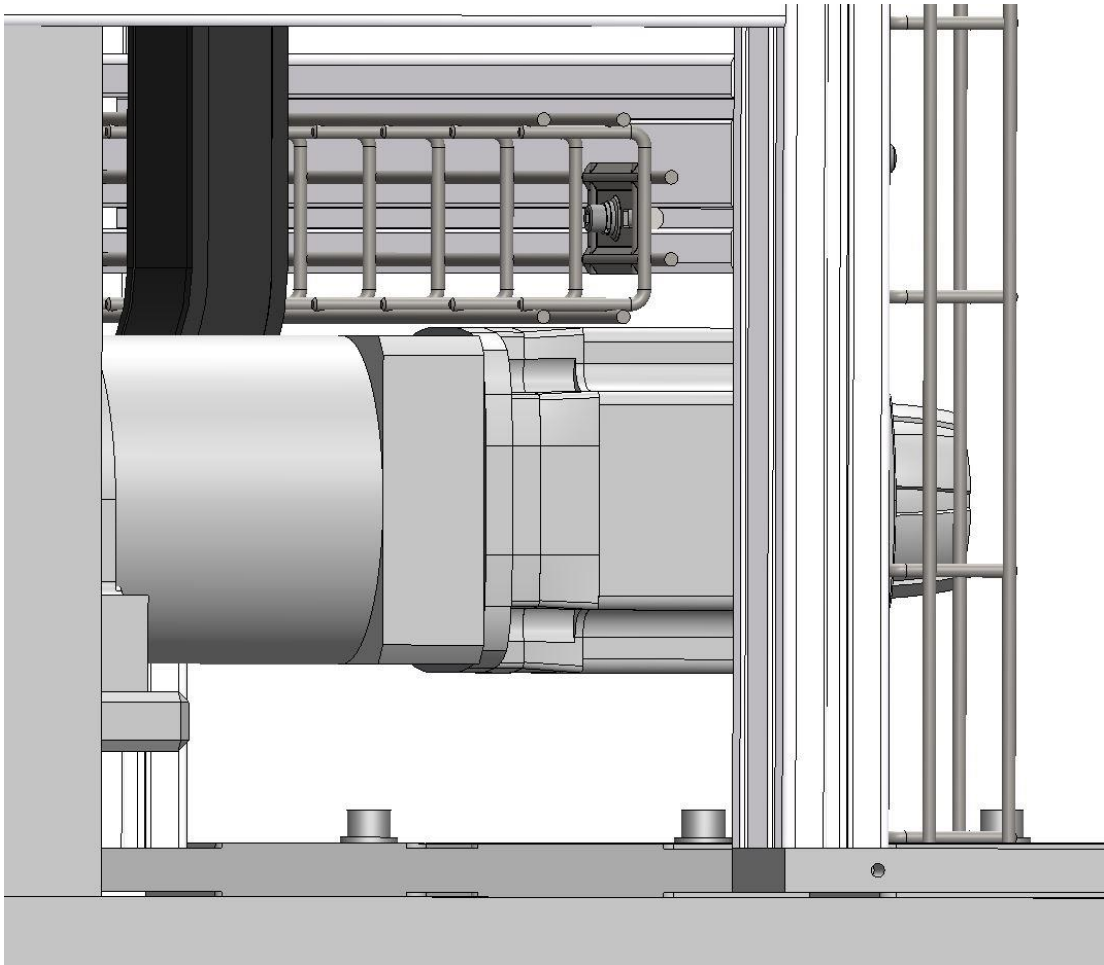


Figure 10. Rear side interference

Interference, as seen in Figure 10, with other pre-made parts of the friction test machine was a significant factor at the modelling phase. Therefore, modelling took considerable time and effort. In the main assembly, there is a beam on the backside of the friction test machine, which holds cables and other equipment. The servomotor would not have fitted under the beam and the cable rail without assembling the force transducer straight to the frame bottom plate. The cable rail can be lifted and attached to the upper slot if it is required to make the servomotor to fit. The servomotor is installed to the same plate that the screw jack system is attached. Although the servomotor is installed offset to the mounting point of the plate and tends to bend the force transducer, it is not regarded as significant because the linear guideways hold against the bending.

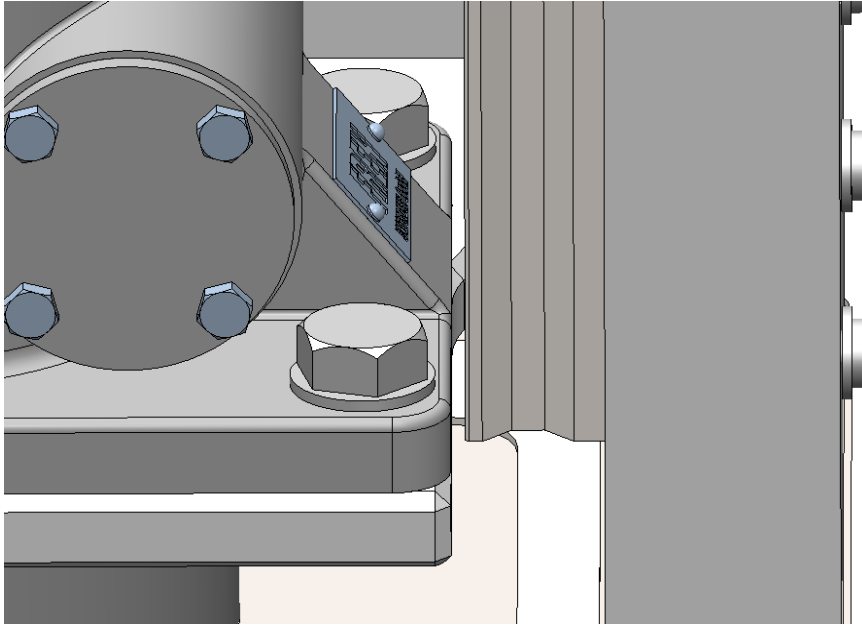


Figure 11. Interference with the screw jack and the right rail

The rail on the right side is sitting very close to the lifted screw system and its attaching plate, but the rail can be cut shorter to avoid collision (Figure 11). The gap between the rail to the plate and the screw jack system is only 3.5 mm on the CAD-model.

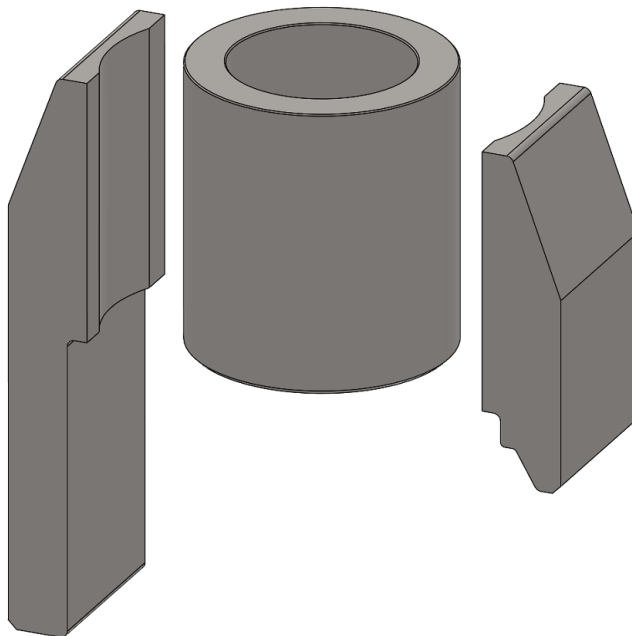


Figure 12. The linear actuator carriage assembly

Thirdly, the designing of the linear actuator carriage was commenced and it was clear after the concepts that it will be constructed from a machined pipe and two thermal cut and pre-machined steel blocks (Figure 12). In order to make the linear actuator carriage as stiff as possible the idea was to add two (2) more Hiwin linear bearing blocks. Due to lifting of the screw jack system there was no space on the right side so the construction was designed with three (3) linear bearing blocks (Figure 13). It was seen to be enough together with tightening the linear bearing blocks to the linear actuator carriage using screws.

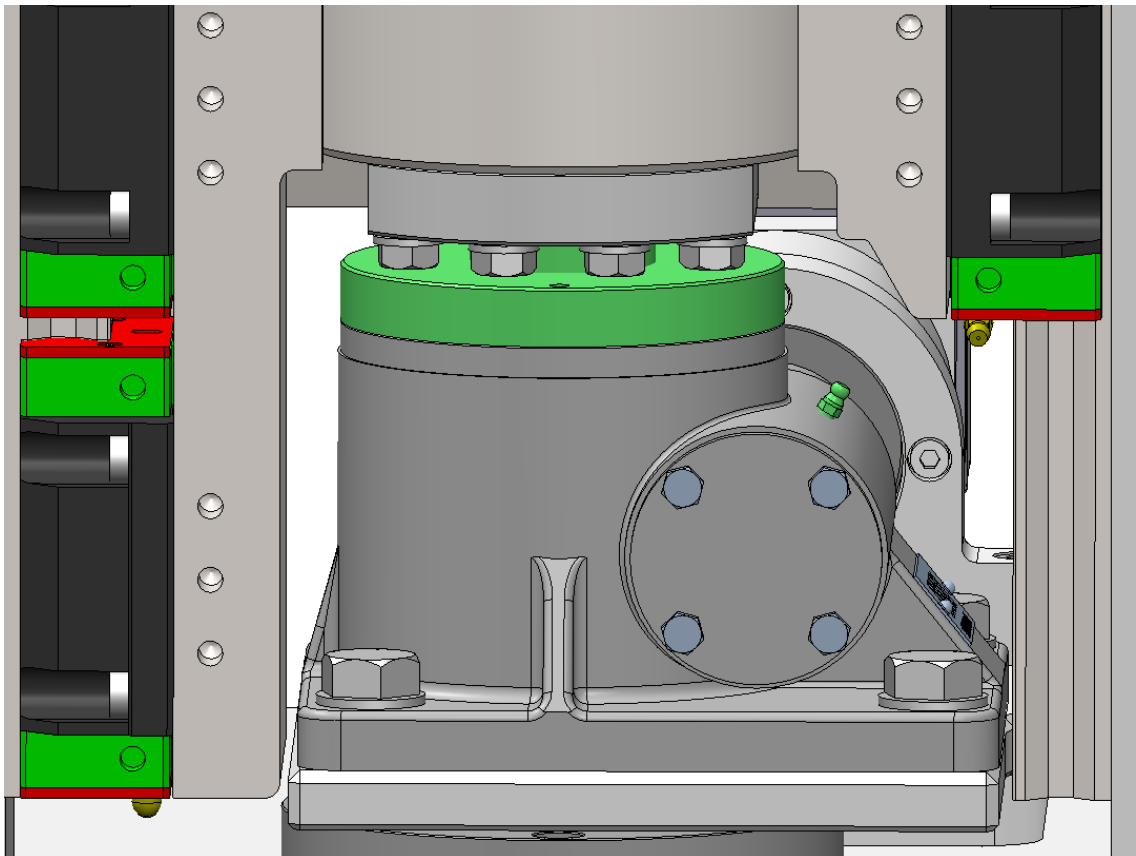


Figure 13. Hiwin linear guideways positioning

After pre-machining the linear actuator carriage parts would be welded together. Next the carriage would be reannealed and machined to the specified tolerances. The pipe was decided to be a hollow bar from Polarputki Oy. The material was selected from Polarputki's catalog to be E420J2 structural steel. The two thermal cut parts' material was chosen to be common structural steel S355J2G3.

The mounting of the linear bearing blocks was then to be revised because they glided against the linear actuator carriage even though on the first revision had shoulder on one side to prevent gliding. The Hiwin RGW45CC linear guideways were chosen already in the first revision of the friction test machine and they were calculated to be strong enough to handle the forces. The linear guideway load ratings can be seen in Appendix 2. The idea of clamps on side of the linear bearing blocks was taken from Hiwin catalog in Appendix 3. The forces were calculated in an event of collision, which is not the desired occasion but an extreme incident.

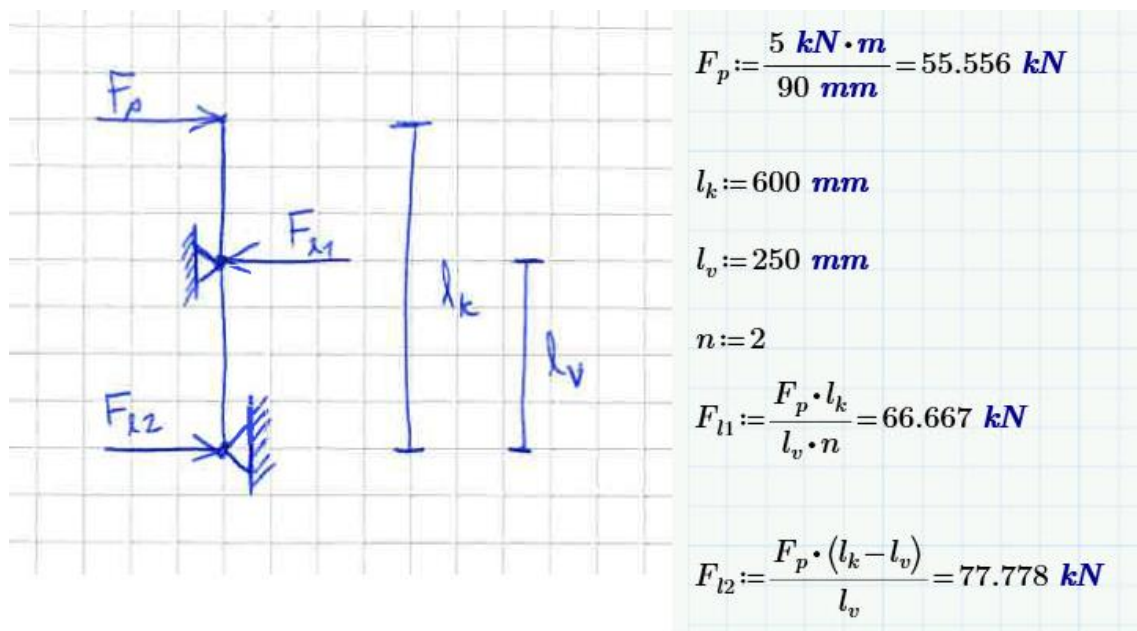


Figure 14. Calculations of the forces to the clamps in a collision

F_p is the force that the rotary specimen will produce in a collision. l_k is the distance from the rotary specimen to the lower linear bearing block. l_v is the distance between the lower linear bearing block and the upper linear bearing block. F_{l1} is the force to each of the upper bearing blocks in a collision event and F_{l2} is the force to lower bearing block at the collision event. (Figure 14.) An M10 Grade 8.8 coarse pitch thread bolt will have a 28 500 N preload force and an M10 Grade 10.9 will have a 41 800 N preload force [5, p. 460]. Three (3) M10 bolts were calculated to be enough to hold the force the clamps could encounter. Three (3) Grade 8.8 bolts would place an 85 500 N preload force and three (3) Grade 10.9 bolts would place a 125 400 N preload force. The bolts were selected to be Grade 10.9 as the forces at the friction test machine may be significant. The

requirements found in AS2 that the nominal slip forces is at least 1.25 times the overall theoretical shear force, as well as the nominal gapping force is to be 1.25 times the theoretical tensional or axial forces are then met. The material of the clamps was selected to be EN 1.4401 Stainless Steel, since no surface finishing or rust protection is needed after manufacturing. The material has high yield strength, which is excellent for the purpose.

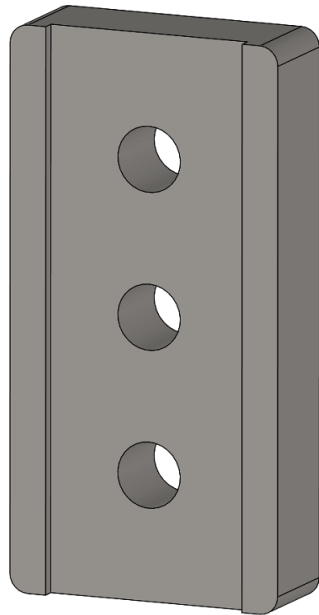


Figure 15. The linear bearing block clamp

The clamp was designed to be 90 mm tall, 45 mm wide and 16 mm thick with a 2 mm cut on the front side, which concentrates the preload forces to the linear bearing block and the linear actuator carriage precisely (Figure 15).

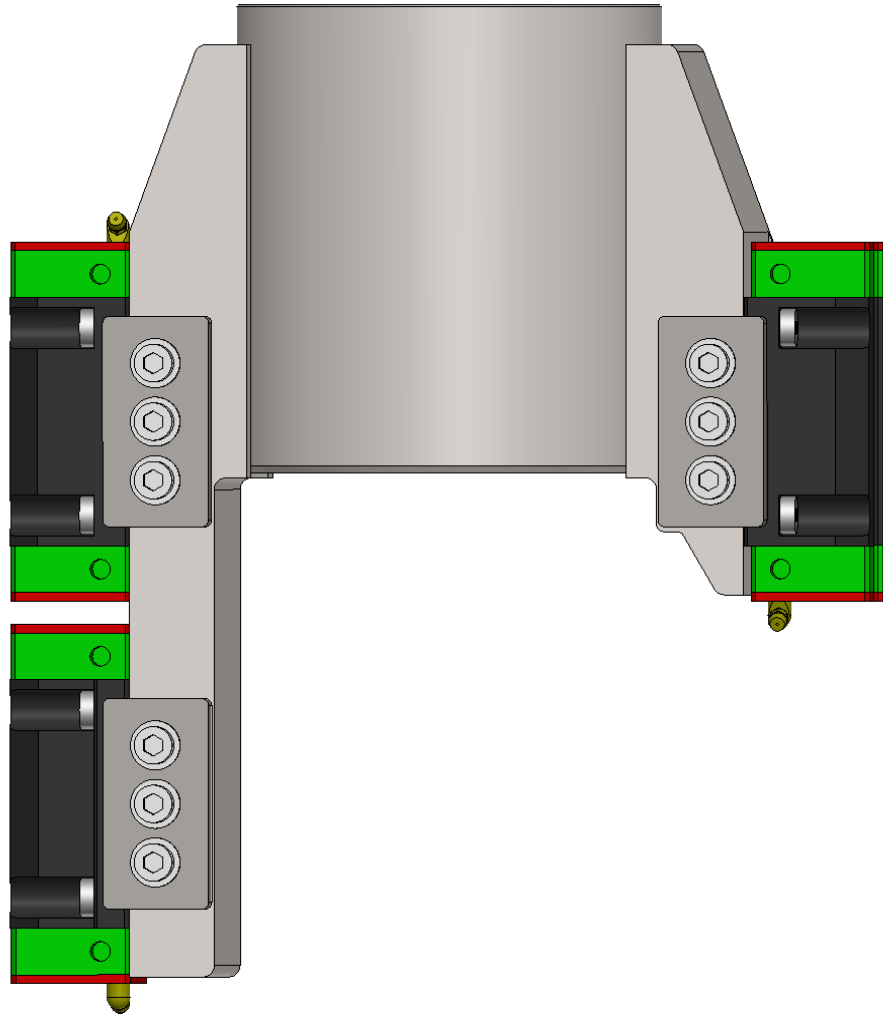


Figure 16. The linear actuator carriage with linear bearing blocks and clamps

The assembly with the linear actuator carriage, the linear bearing blocks and the clamps can be seen in Figure 16.

Finally, the support, which is a load bearing component, required some redesigning and updating to fit the new linear actuator carriage. The first revision of the support could not be modified and used in the second revision, therefore it was redesigned. It was previously made from EN 1.4401 material hence it was the material by default to be used in the redesigned component. The support was attached with six (6) DIN 915-45H socket dog point set screws and two (2) DIN 7979 dowel pins. The dowel pins were calculated to bear all the shear forces involved in the event of a possible collision. The simulation

results indicated that a minimum of two (2) over 5.81 mm solid pins would take all the bending and shear forces. The calculations can be found in Appendix 4. The chosen pins have a thread on one end to ease replacement in case they are damaged or require replacement. The overall diameter of the pins is 8mm, which has a higher cross section than the minimum required, even though the shear forces and plane goes through the section of the pin, where there is the internal thread. The support was designed to be as low and stiff as possible from the plane where the rotary specimen interfaces to the interfacing surface between the support and the linear actuator carriage (Figure 17).

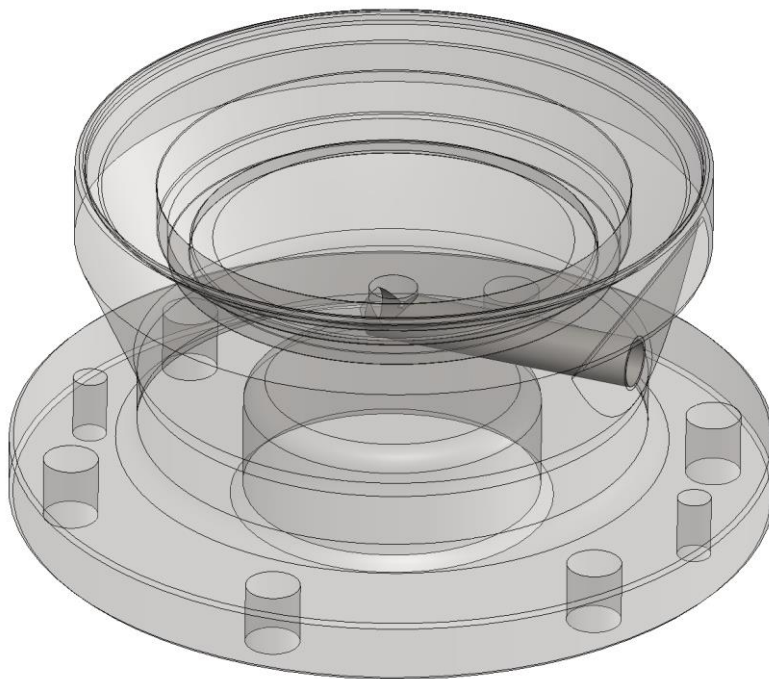


Figure 17. The support

Some functional features on the support are the test pressure inlet from the side of the support to the middle and beneath the support a counter bore for clearance the screw jack ball thread. The dowel pins were positioned to the sides to divide the loads steadily and positioning the support in the center of the linear actuator carriage.

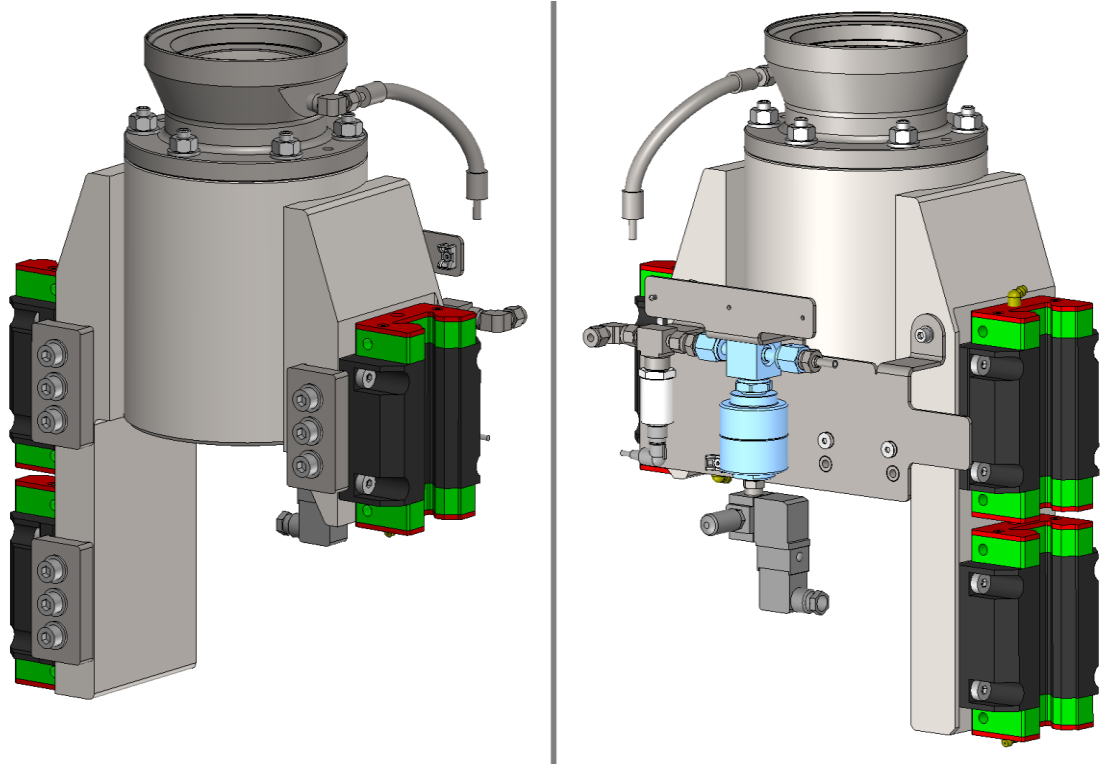


Figure 18. The redesigned linear actuator carriage assembly

Figure 18 illustrates the redesigned linear actuator carriage assembly with the linear bearing blocks, the support, the clamps and some components for the pressure testing subassembly.

3 Simulation

3.1 FEM Boundary Conditions

The forces computed were to be checked against standards AS1, AS2 and AS3 in Table 1. The purchased components must have a positive margin of safety with regard to the nominal design loads of the components.

Initially, the purpose was to make the analysis based on the entire model, which will fulfil the requirements of the mentioned standards. Several iterations were made, to have a more accurate understanding of what was happening in the structure while loading. All conditions calculated were normal conditions of use for maximum loads, which were pre-defined when the friction test machine was designed. For all critical parts, as seen by machinery safety and reliability, needed to be calculated and documented as per requirements in the previously mentioned standards.

Regarding fatigue, it is considered highly misleading to carry out any fatigue analysis using the possible history of the system, due to the fact that the differences in loads and test conditions are foreseen to change considerably during the lifespan of the friction test machine. The fatigue standard is taken into consideration as per the main guidelines and allowable stresses in structural steel, rather than the accurate calculation of the fatigue.

3.2 FEA Simulations and Results

The first FEA (Finite Element Analysis) simulations were carried through SolidWorks Simulation. It was a fluent way to begin the simulations because the assembly was made with the same software and there was knowledge of the simulation software at this department of Rejlers. There are many positive features in the simulation software, however, after a couple of weeks of learning the simulation side of the SolidWorks 2018, it was still uncertain that the results were correct and if the applied torque had a correct effect. Also the calculation lasted sometimes over 24 hours and it was not certain that the simulations would succeed because the SolidWorks Simulation progress window did

not give any relevant information than just a percentage number which would not change for hours. (Figure 19.)

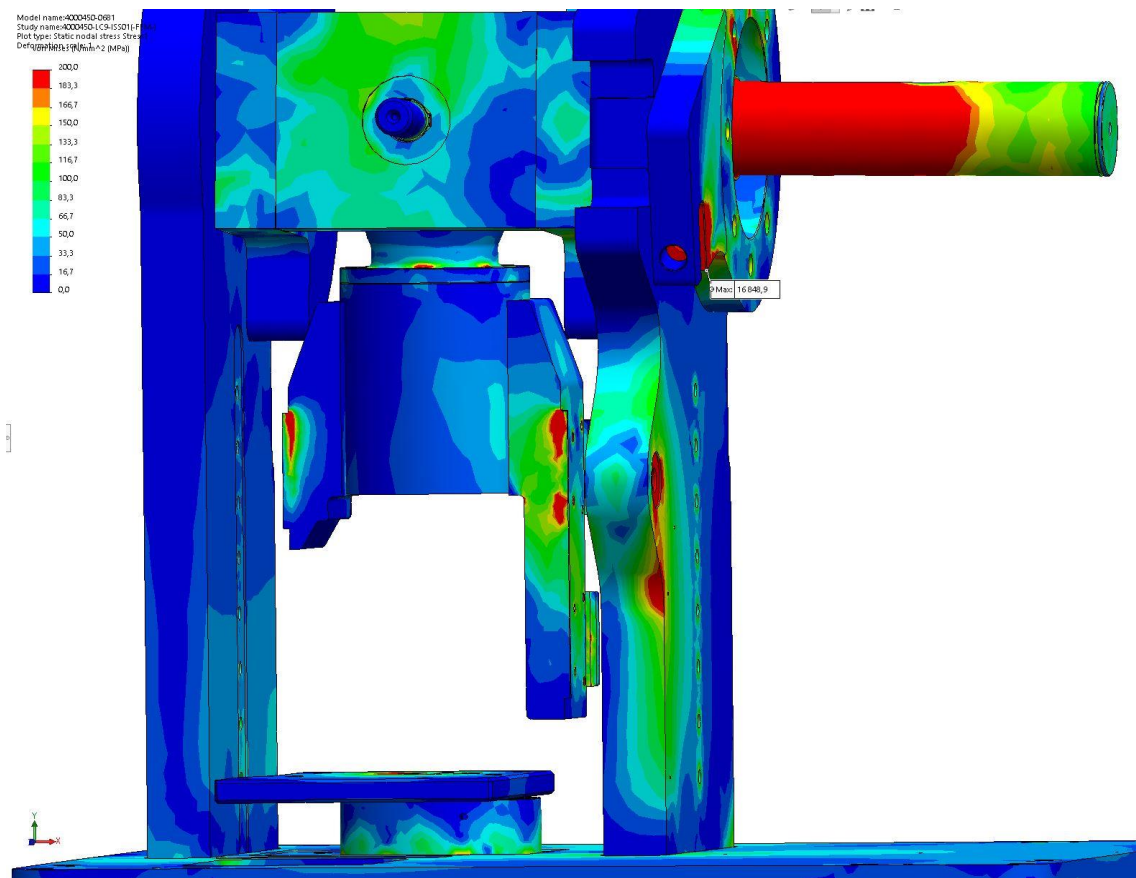


Figure 19. Uncertain stress results from SolidWorks Simulation

Ansys was taken in to use on the simulations, because it calculated significantly faster and provided faster iterations between analyses, even though some studying of the software was required, do that the boundary conditions represented the real conditions as accurately as possible. The results from Ansys simulations were significantly constant and the torque was affecting correctly. (Figure 20.)

J: 4000450-0681 w/ BOLTS smalltol 23 frictionless smaller mesh

Equivalent Stress

Type: Equivalent (von-Mises) Stress

Unit: MPa

Time: 2

11.11.2019 18.57

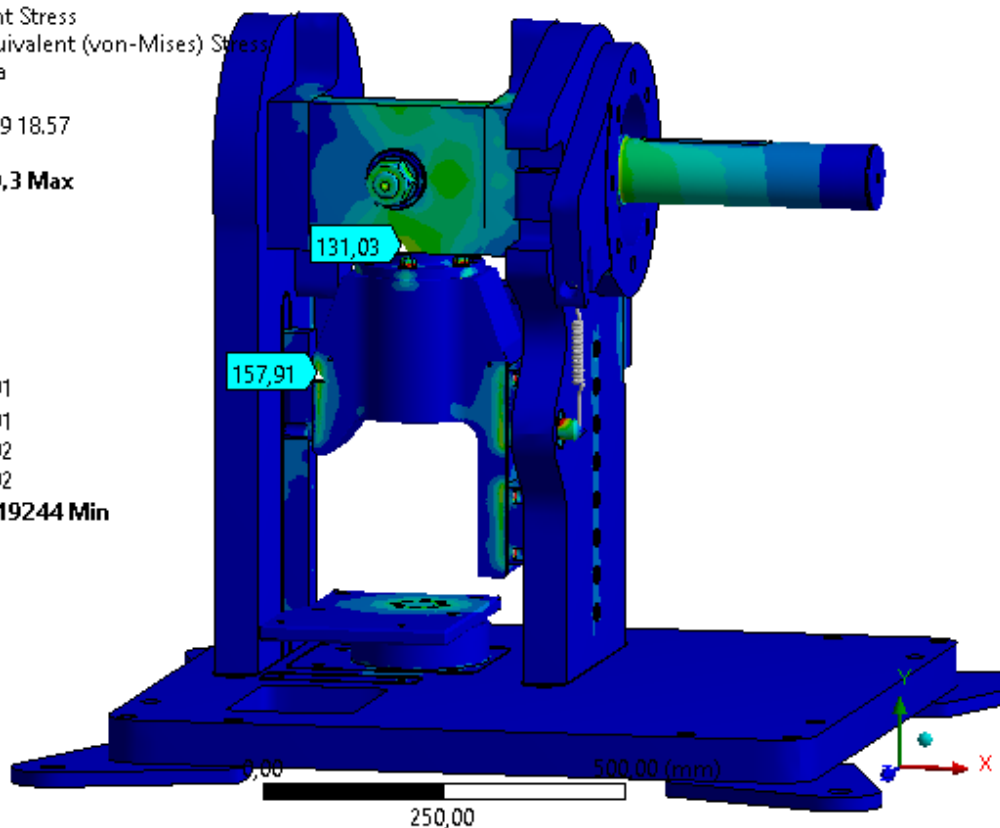
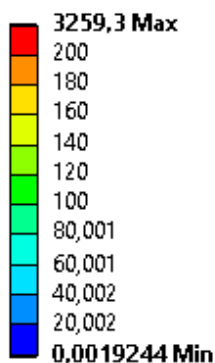


Figure 20. Stress results from Ansys Mechanical simulation

Maximum forces used in the analysis of the friction test machine are 100 kN pressing force from the screw jack system and at the same time 5 kNm torque from the cradle axle. In simulations, the forces were 150 kN pressing force and 8 kNm torque which are more than 1.25 times the maximum forces designed to be used. The rotary specimen and the plane were bonded together in the simulations for analyzing the event of collision. The material used in the simulations was structural steel as the Young's Modulus of 200 GPa is similar to all the parts used in the simulations. The used element order was set to "Program Controlled" in Ansys, and with that setting, Ansys solved the simulation model with SOLID186 elements and SOLID187 elements which are quadratic element order conducted to 3D SOLID models.

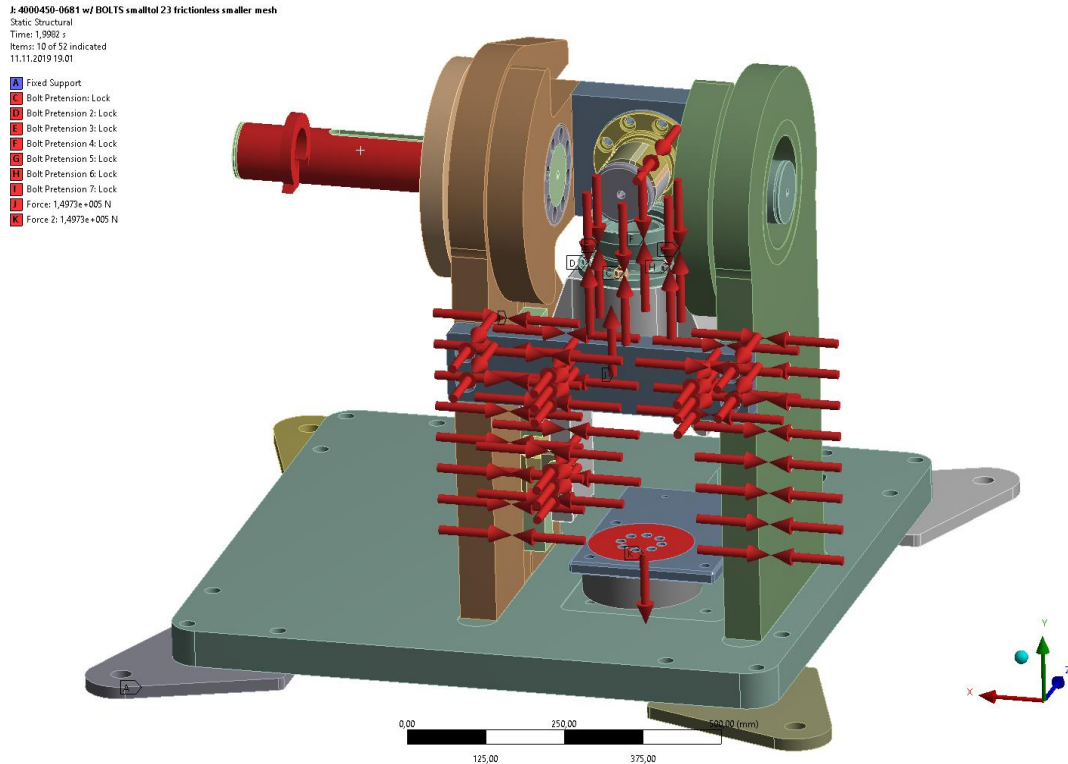


Figure 21. Bolt preloads, screw jack forces and cradle moment

The simulation model was shaped as simple as possible to perform the simulations as efficiently as possible and still accurate. Ansys has a function to perform automatic connections with a specified tolerance. The tolerance used was 0.2 mm and it gave 185 connections. Ansys specifies the automatic connections as bonded and the connections were modified to properly reflect the connections. The cradle bearings were simulated with Ansys bearing connections. Instead of the force transducer measuring the torque, a very stiff spring was used that allowed to study the force applied to the force transducer. The simulations were done with two (2) load steps. Critical bolted connections were built with beam connections in Ansys Mechanical and the connections were preloaded with specified forces [5, p. 460]. The preload forces of the beams were applied in the first load step and the force was locked in the second load step. (Figure 21.) A frictionless connection was set between the parts with simulated bolted connections. Also a frictionless connection was applied between the linear bearing blocks and the linear guideway rails. [6.]

On the second load step the screw jack forces of 150 kN to the bottom of the linear actuator carriage and top of the screw jack system attachment plate and moment of 8 kNm to the shaft of the cradle were applied. The first iterations were done with a larger mesh size. The mesh had 790 000 nodes and 421 000 elements. These allowed the simulation results to be available in 3 to 15 minutes depending on the connection types used. Using only “Bonded” and “No separation” connection types were calculated faster and when frictionless was used in appropriate connections, solutions were more slowly calculated.

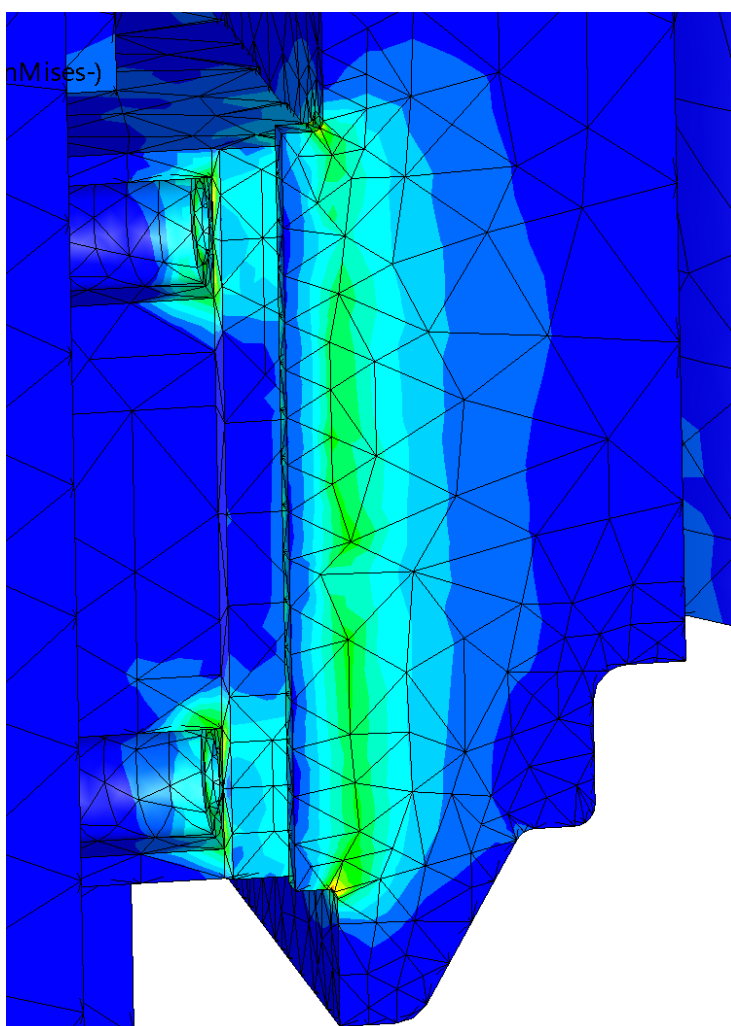


Figure 22. Results from first few iterations

After the first few simulation iterations, the model had to be modified since the stress spikes at the corners of the linear bearing blocks' shoulders as seen in Figure 22. Stress

spikes to those corner areas were suspected to fracture due to fatigue. The shoulders were revised to be continuous from top to bottom.

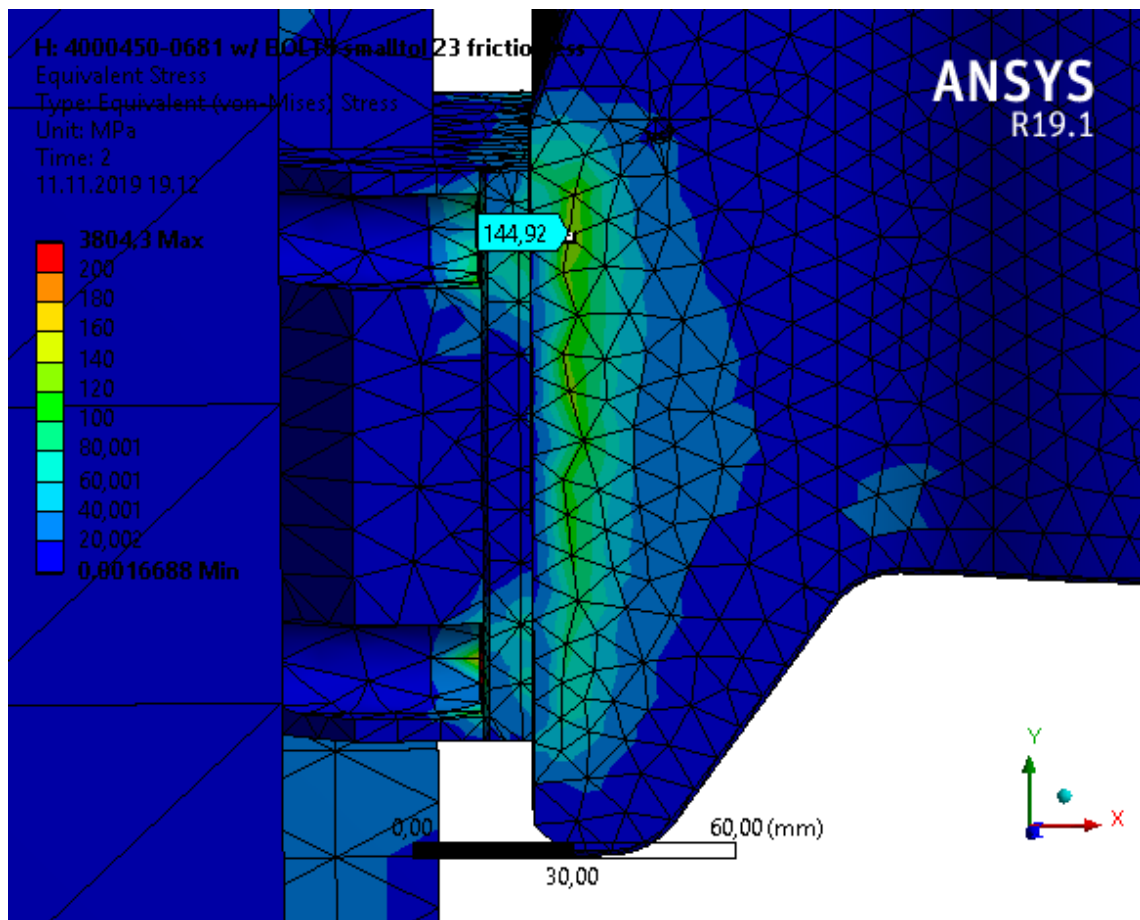


Figure 23. Modified shoulder area

Modifications to the shoulder area lowered the stresses and no stress spikes occurred after (Figure 23). The stresses in the shoulder area were maximum of 145 MPa which is less than half of 355 MPa, the minimum yield strength of the S355J2G3. Results convinced after few tenths of iterations with Ansys and the mesh was optimized on the areas which pointed out to require more explicit mesh as seen in figure 24. The mesh in last iterations was made with 2 624 000 nodes and 1 729 000 elements. The results were calculated in less than 7 hours, which is considerably less than SolidWorks Simulation software calculated with a far lower volume mesh.

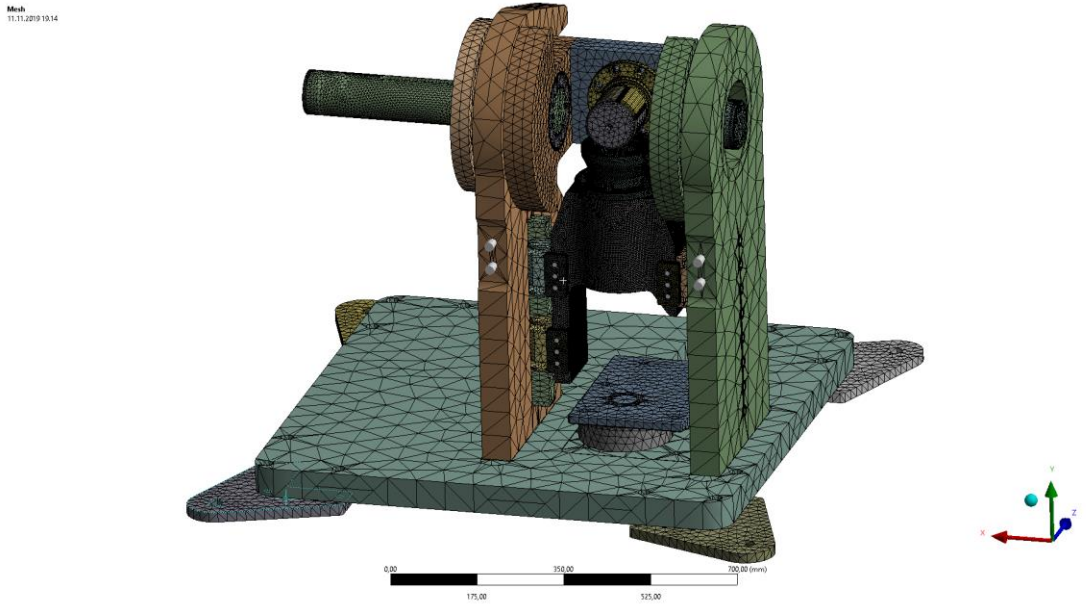


Figure 24. Optimized element quantity on critical areas

The results were slightly changed with the optimized mesh. The maximum stress were reduced. The stresses lowered in some parts and in other parts increased as the results became more precise.

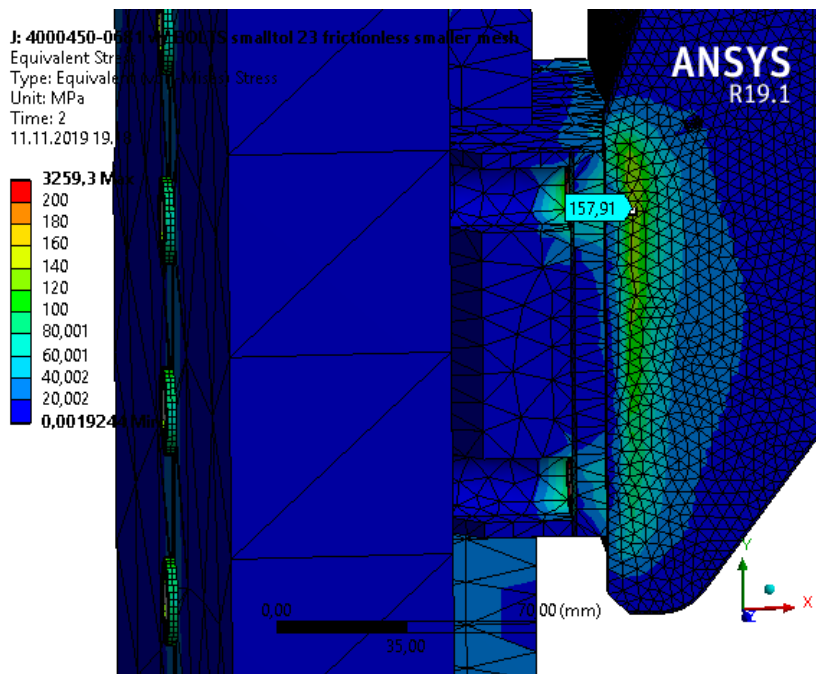


Figure 25. Maximum stresses increased

As seen in Figure 25, the maximum stresses in the shoulder area were increased by 13 MPa to 158 MPa in total which still produces a safety factor of over 2. The stresses of over 3000 MPa came from the bonded contact between the rotary specimen and the plane and are not regarded as critical to the designed construction.

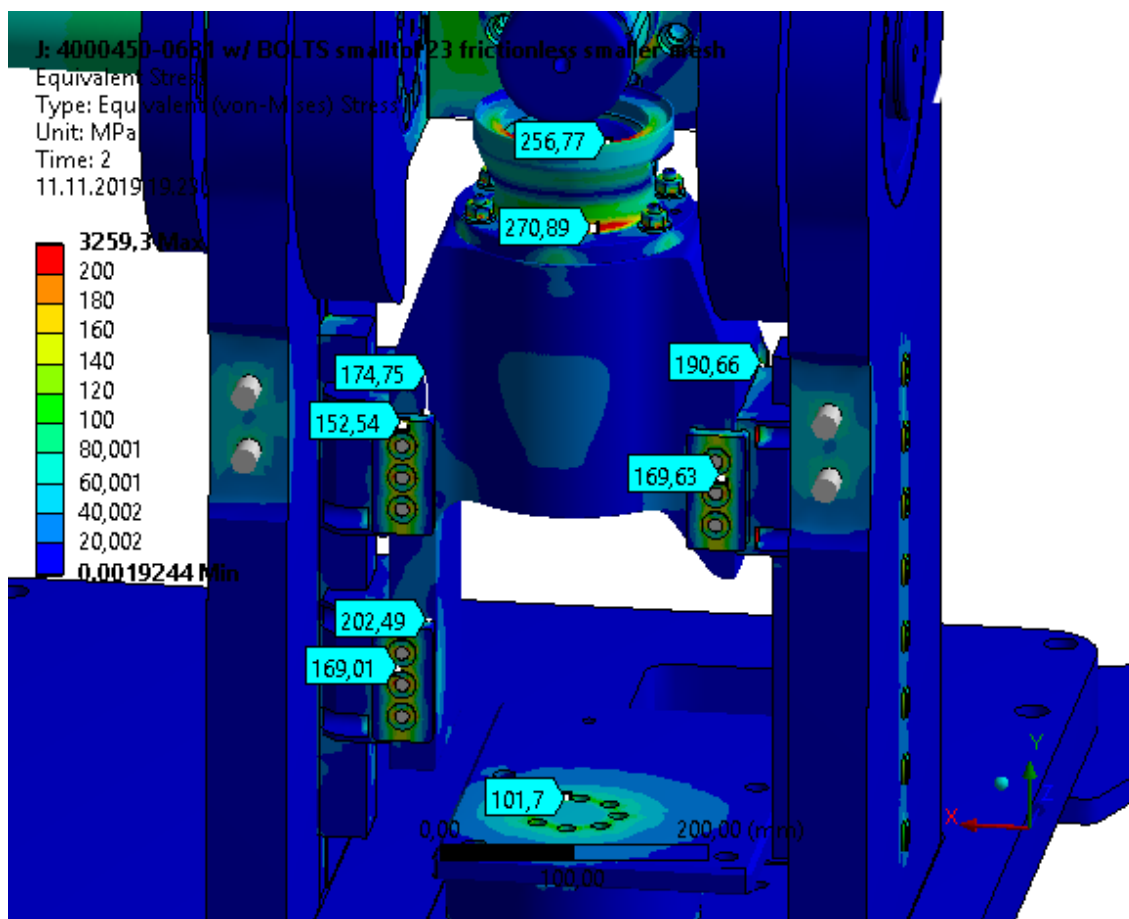


Figure 26. Maximum stresses at front side

On the front side, maximum stresses of 270 MPa to the support occur to the lower part of it. The stress is compressive and it is designed to be the breaking point if the pins and bolts holding the support to the linear actuator carriage do not break before. Maximum stresses of 202 MPa to the clamps are reasonable and are caused by contact pressure. Maximum stresses of 102 MPa to the screw jack plate are also decent. Maximum stresses of 190 MPa on the linear actuator carriage against the linear bearing blocks are acceptable from the contact pressure. (Figure 26.)

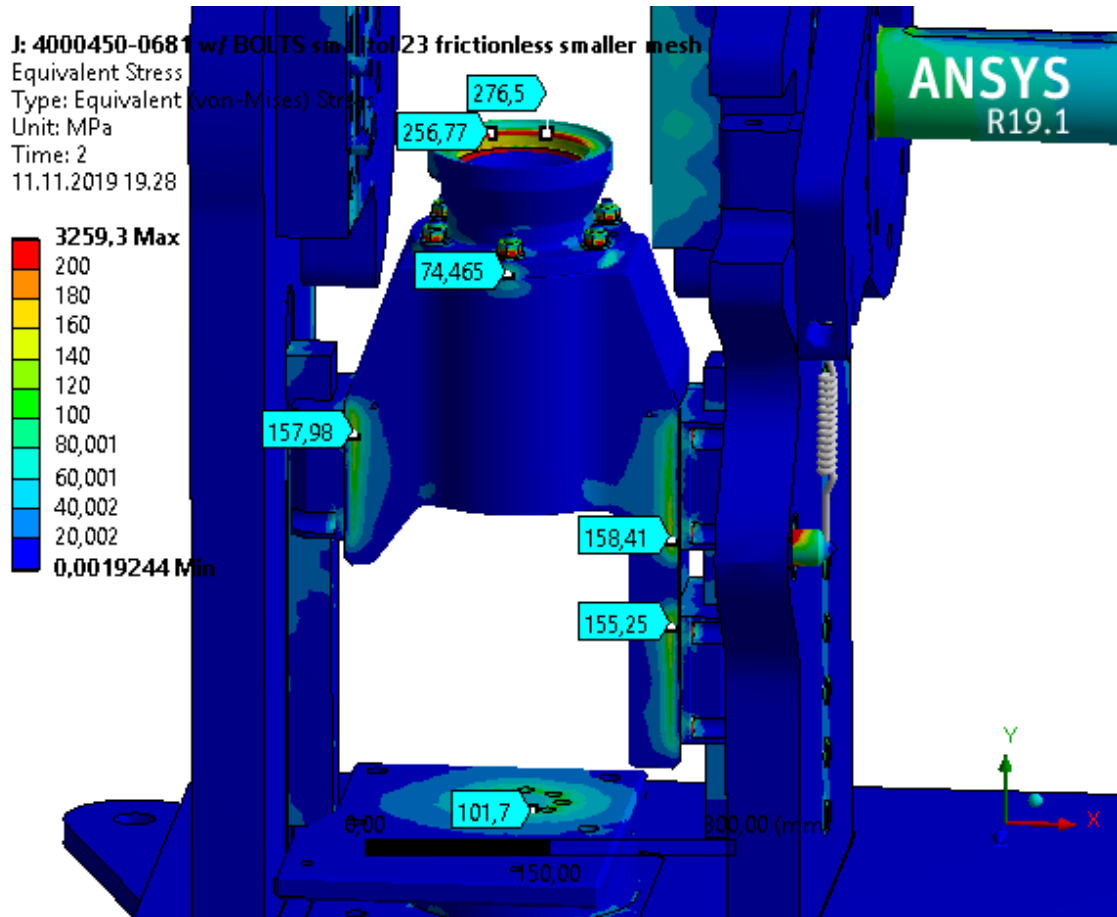


Figure 27. Maximum stresses at back side

In Figure 27 from the backside of the friction test machine, maximum compression stresses of 277 MPa to the front inner edge of the support are visible and caused by the extreme forces on the simulation which do not occur on normal operations of the friction test machine. The stresses of 158 MPa to the linear actuator carriage on the backside are reasonable and caused mainly from the pretension of the linear bearing blocks with the clamps. All the stresses have a safety factor of more than 2 and the forces used in the simulations are over 1.5 times of maximum permissible forces.

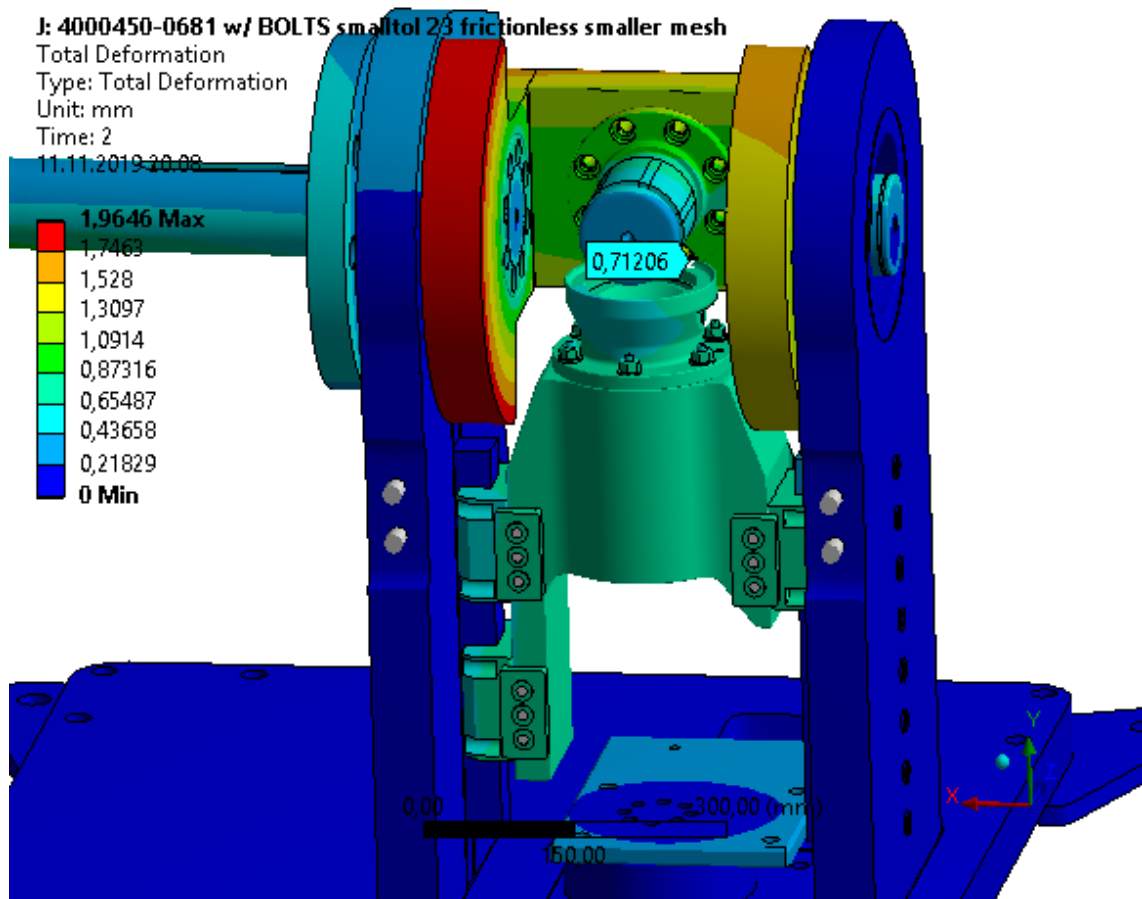


Figure 28. Total deformation

Total deformation of 0.71 mm is primarily along the Y-axes of the simulation model in Ansys seen in Figure 28. The linear actuator carriage, the support, the clamps and the linear bearing blocks move up on the rails as there is a frictionless contact between the linear bearing blocks and the rails.

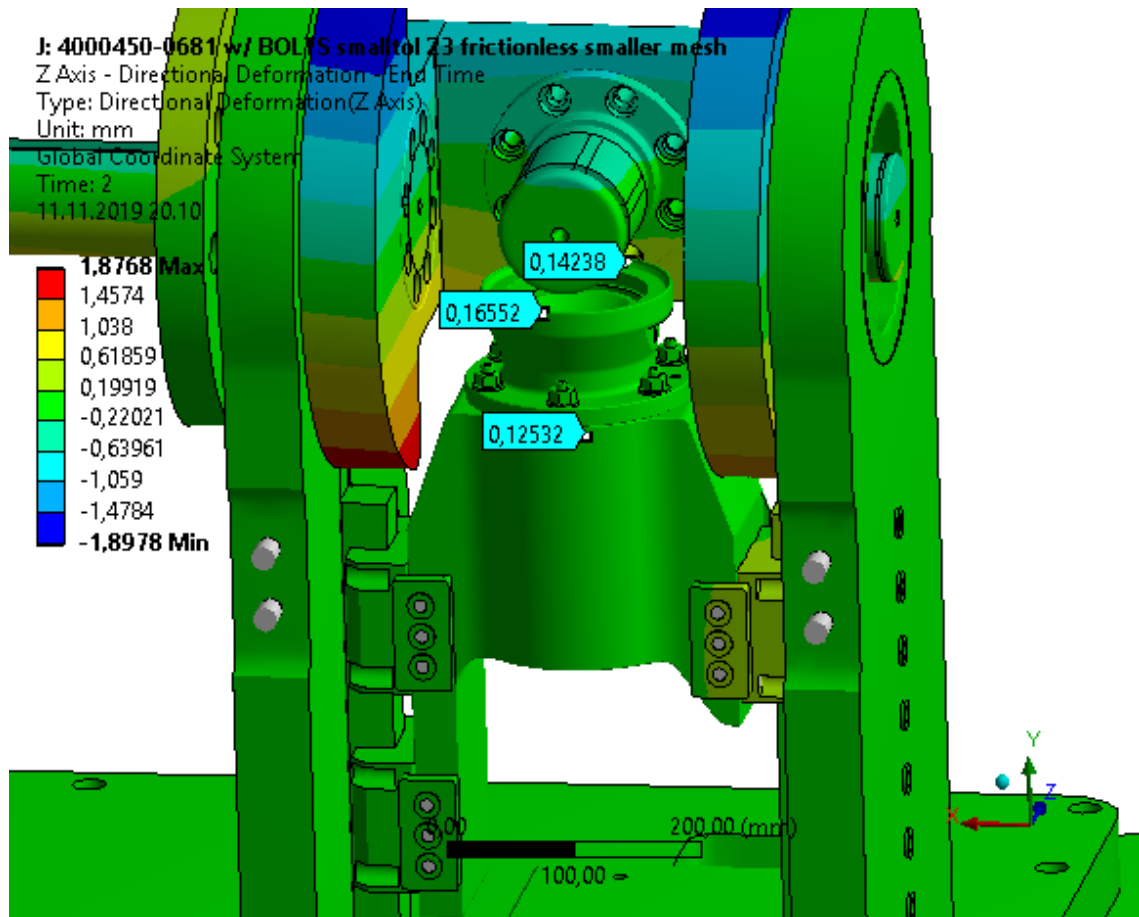


Figure 29. Z-axes deformation

In the Figure 29, the deformation of the linear actuator carriage and the support along the Z-axes is considerably less than the total deformation. Deformation of 0.17 mm on the Z-axes at the support edge is permissible considering the forces applied to the friction test machine on the simulation. The linear actuator carriage together with the support can be considered stiff after the redesigning.

4 Manufacturing

Firstly, the linear actuator carriage was to be built from three (3) pieces. In the center, there would have been a pipe pre-machined in length, inside and outside diameter prior to welding. The steel blocks attached to the pipe would have been thermal cut and pre-machined before reannealing. Lastly, the linear actuator carriage would have been machined to the specified tolerances.

All the drawings were made including tolerances and manufacturing standards. The drawings are included in Appendix 5. One of Rejlers trusted subcontractor was invited to submit a bid of the linear actuator carriage. Rejlers provided files containing all the drawings and CAD-models of the redesigned parts. The subcontractor was given free hands with a tight schedule. The subcontractor submitted a bid to do the linear actuator carriage from one (1) piece with their 5-axes milling machine. The tight tolerances are easier to achieve when manufacturing the linear actuator carriage without welding. The distortion from welding large pieces may cause challenges, now it can be avoided significantly with machining from one (1) piece. Minor modification was done to the linear actuator carriage prior to machining, and the modifications allowed preferable machining (Figure 30).

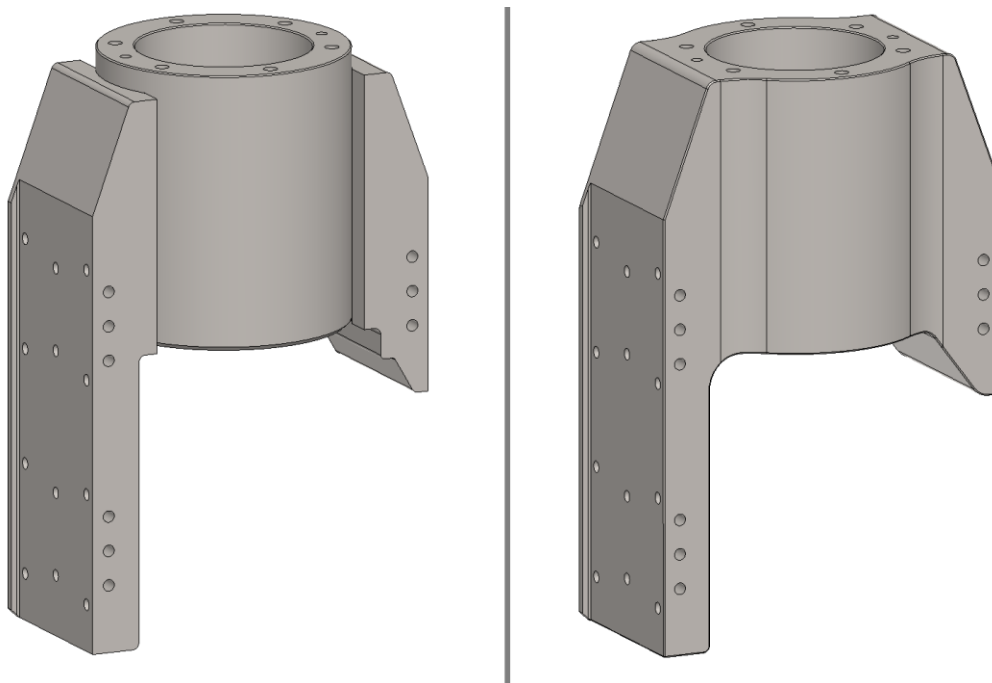


Figure 30. The linear actuator carriage: On the left welded model and machined on the right

Figure 31 illustrates the machining process of the linear actuator carriage in 5-axes machining center. The steel billet block weighed almost 200 kg and the machined linear actuator carriage weighed 45 kg.

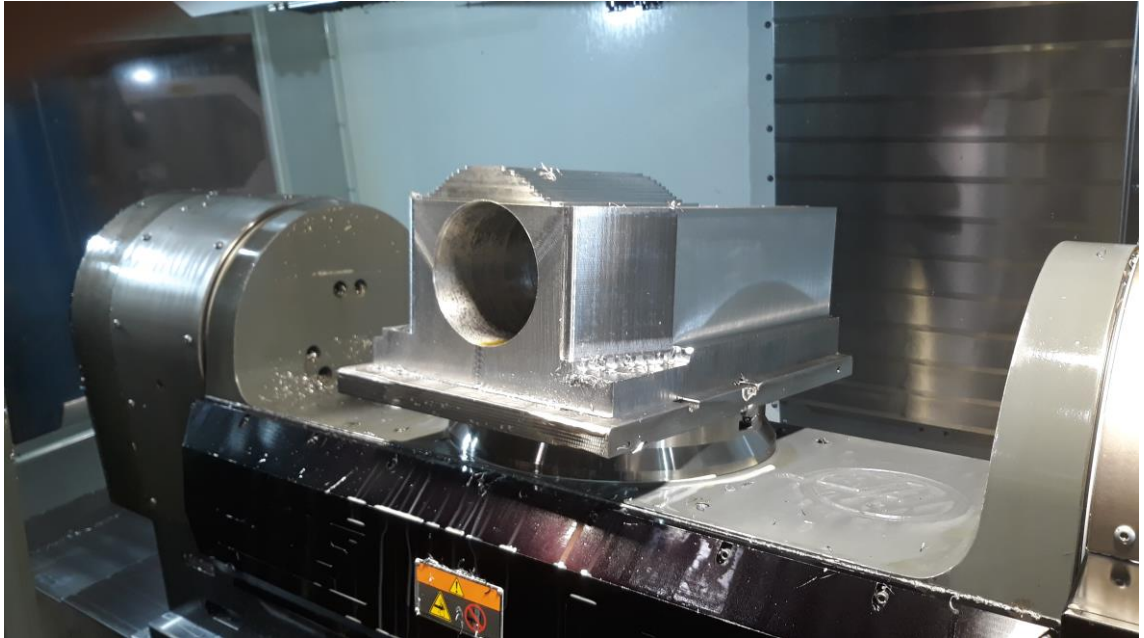


Figure 31. Machining process [7]

The project schedule was 5-6 weeks, and the new mechanical design and components are available for assembly at Rejlers AIT (Assembly, Integration and Test) facility located at Rejlers supplier in Järvenpää. The testing will be subsequently made after the mechanical installation, and will conclude the commissioning of the friction test machine to the end clients.

5 Conclusion

The main goal of this thesis was to redesign the friction test machine, which had a compatibility problem with the PID adjustment of the screw jack system. Also, the linear actuator carriage was too flexible due to the force transducer placement. The aim was to limit the changes to the minimum number of parts, which added to the challenge as the machine was already manufactured. In addition to the tight schedule, the challenge of the thesis was increased by the change of the simulation software during the thesis and the use of new tools in the software. The topic involved a variety of problems that required inventiveness and acquiring new knowledge.

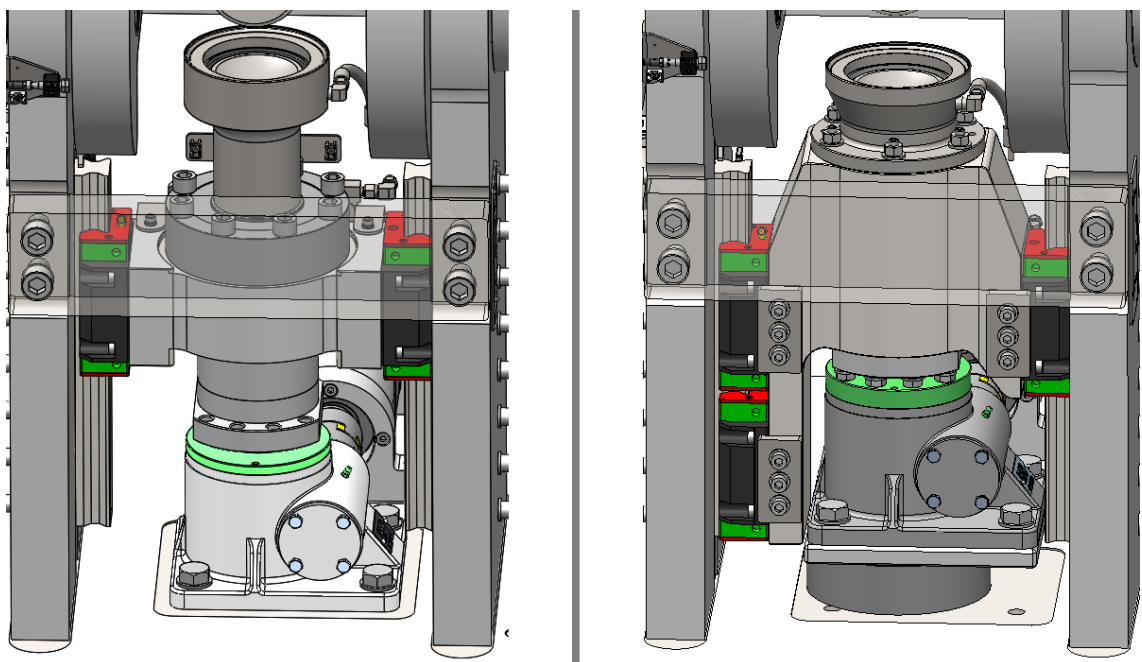


Figure 32. The original design on the left and the redesigned machine on the right

A suitable solution was found which required the modification of one (1) part, and the manufacturing of four (4) new components (Figure 32). The screw jack system was changed to a reversible model to work with PID control. The force transducer was moved to the lowest position in the assembly where it cannot bend. A plate was designed on the force transducer to attach the screw jack system to the force transducer. On top of the screw jack system, the linear actuator carriage was redesigned to be stiffer by the addition of a single linear bearing block. The linear bearing block increased the linear

actuator carriage torsional stiffness. The support was redesigned on the linear actuator carriage, which was also made as stiff as possible.

Based on the results of the simulations, the stiffness of the friction test machine was significantly increased, which provides the basis for a functioning machine. Changes in the screw jack system make the PID adjustment work, so that the forces remain within the controlled range and the friction does not increase too much to bend the structure. Bending less than 0.17mm in the Z-axis with very high forces is a very big improvement over the original design. With a safety factor of more than 2 for maximum stresses, the structure is also encouraging.

The goals of the thesis were achieved well, although learning the simulations with a large assembly was challenging and the schedule was tight. Next, the friction test machine will be dismantled for replaceable parts and the redesigned parts will be replaced. The commissioning will then be carried out and the force sensor scale will be calibrated. Once the required tests have been completed, the friction test machine is handed over to the clients. Thanks to the engineering process, the use of Ansys was discovered to be more efficient and optimized for the parts designed.

References

- 1 HBM Force Transducer. 2019. Web source. HBM Finland. <<https://www.hbm.com/en/2409/u5-robust-load-cell-for-tensile-and-compressive-forces/>> Accessed October 11, 2019.
- 2 Milled blanks. 2019. Web source. Fodesco Oy. <www.fodesco.fi/main.php?sub=shop&nav=webshop&id=15494> Accessed October 15, 2019.
- 3 Hiwin Linear Guideways. 2019. Web source. Hiwin GmbH. <https://www.hiwin.de/en/Products/Linear_Guideways/Series_RG_QR/Block_RG/RGW/4359/2443819> Accessed October 10, 2019.
- 4 Hiwin Linear Guideways GW-10-3-EN-1708-K.pdf. 2019. Web source. Hiwin GmbH. <<https://www.hiwin.de/en/Dokumente.html>> Accessed October 12, 2019.
- 5 Prof. Dr.-Ing. Harald Meerkamm. 1st edition, 2014. Schaeffler Technical Pocket Guide. Schaeffler Technologies GmbH & Co. KG
- 6 Simulating Bolted Assemblies. 2019. Web source. Ansys, Inc. <<https://www.ansys.com/products/structures/strength-analysis/simulating-bolted-assemblies>> Accessed October 15, 2019.
- 7 Fab-Pro Metalworks. 2019. Picture. Accessed November 8, 2019.

HBM Force Transducer Data Sheet [1]



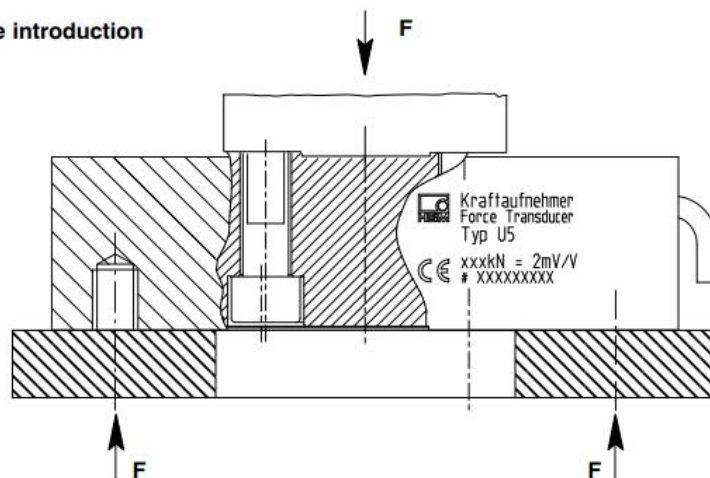
View from below

U5 Force Transducer

Special features

- Tensile / compressive force transducer
- Nominal forces 100 kN ... 500 kN
- Variable installation options
- Flange connection can be centered on both sides
- Low overall height
- High transverse force stability

Force introduction



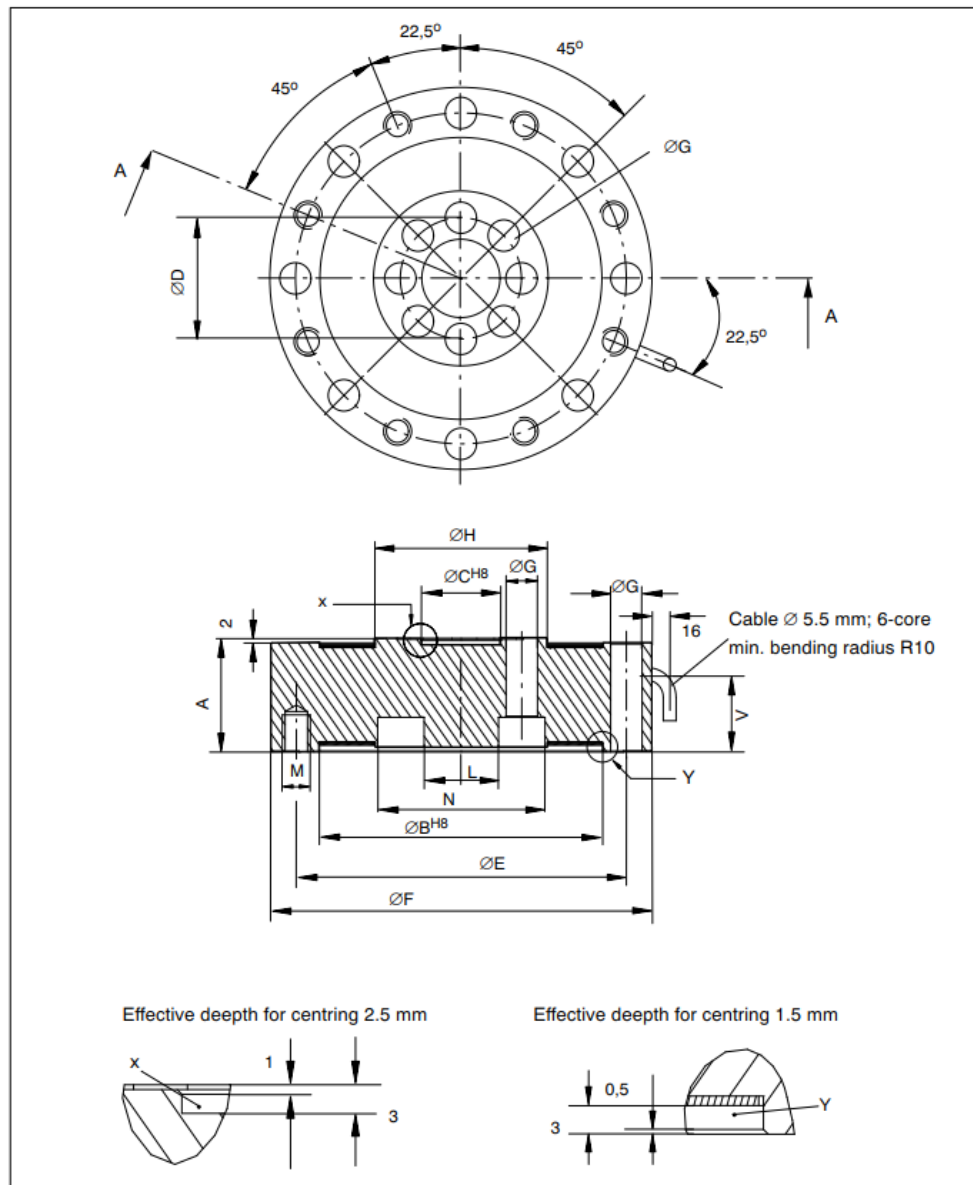
B0793-4.3 en



Specifications (VDI/VDE 2638)

Nominal force	F_{nom}	kN	100	200	500
Accuracy class			0.1		0.3
Nominal sensitivity	C_{nom}	mV/V	2		
Rel. sensitivity deviation compressive force	d_C	%	< ± 0.25		
Rel. tensile/compressive force sensitivity difference	d_{zd}	%	< ± 0.2 (typically 0.07)	< ± 0.5 (typically 0.02)	< ± 2 (typically 1)
Compressive force sensitivity difference when using through-holes on the outer ring	d_{dd}	%	< ± 0.2 (typically 0.07)		< +1 (typically 0.5)
Rel. deviation from zero	$d_{s,0}$	%	< 1		
Rel. range of inversion (0.5 F_{nom})	$u_{0.5}$	%	< 0.2		
Linearity deviation compressive force	d_{lin}	%	< 0.1		
Linearity deviation tensile force	d_{lin}	%	< 0.1		< 0.3
Effect of temperature on sensitivity/10 K by reference to sensitivity	TK_C	%	0.1		
Effect of temperature on zero signal/10 K by reference to sensitivity	TK_0	%	0.1		
Effect of transverse forces (t. force 10 % F_{nom})*	d_Q	%	< ± 0.1		
Effect of eccentricity / mm		%	< ± 0.1		
Rel. creep over 30 min	d_{crF+E}	%	< ± 0.05		
Input resistance	R_e	Ω	> 345		
Output resistance	R_a	Ω	300 - 400		
Isolation resistance	R_{is}	Ω	> 2x10 ⁹		
Reference excitation voltage	U_{ref}	V	5		
Operating range of the excitation voltage	$B_{U,G,T}$	V	0.5 to 12		
Nominal temperature range	$B_{t,nom}$	°C	-10 to +70		
Operating temperature range	$B_{t,G}$	°C	-30 to +85		
Storage temperature range	$B_{t,S}$	°C	-50 to +85		
Reference temperature	t_{ref}	°C	+23		
Max. operational force	(F_Q)	%	150		
Limit force	(F_L)	%	150		
Breaking force	(F_B)	%	> 300	> 250	
Static lateral limit force	(F_Q)	%	60	50	
Per. torque	M_g	kN-m	1	2	5
Nominal displacement	S_{nom}	mm	0.09	0.11	0.16
Fundamental resonance frequency	f_G	kHz	4.8	4.3	3.3
Weight		kg	5	7	17
Rel. permissible vibrational stress	F_{rb}	%	160		100
Degree of protection to DIN EN 60529			IP65		

* by reference to a force introduction point on the force-introduction surface



Nominal force	A	ØB ^H	ØC ^H	ØD	ØE	ØF	ØG	ØH	V	M	L	N
100 kN	49	122	34	52	142	164	13.5	74	33.5	M12 x 15.5 deep	32	72
200 kN	55	144	43	67	166	190	17	96	37.5	M16 x 19 deep	41	93
500 kN	65	186	76	104	225	260	21	140	48	M20 x 23 deep	72	136

B0793-4.3 en

3

HBM

Order code:

Code	Option 1: Measuring range
100K	Measuring range 100 kN
200K	Measuring range 200 kN
500K	Measuring range 500 kN

Code	Option 2: Electrical connection
K	with cable, 6 m, free ends
M	with cable, 6 m, MS connector (male)
D	with cable, 6 m, D15 connector
Y	with cable, any length, max. 20 m, free ends
N	with cable, any length, max. 20 m, MS connector (male)
F	with cable, any length, max. 20 m, D15 connector
P	with Binder 723 connector

K-U5- [] [] [] [] - [] [] [] [] m

Accessories (also available):

Cable / Connector

Connection cable Kab139A-6, 6 m,
with cable socket 423 and free ends

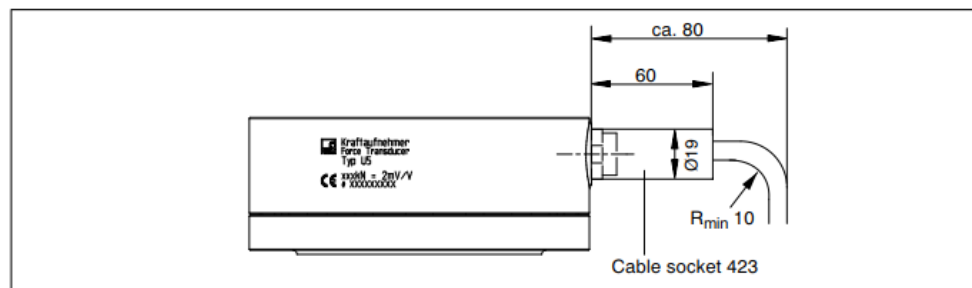
Order number: 1-KAB139A-6

Connector MS3106PEMV, mounted on Kab139A-6

Order number: D-MS/MONT

15-pin D-connector, mounted on Kab139A-6

Order number: D-15D/MONT

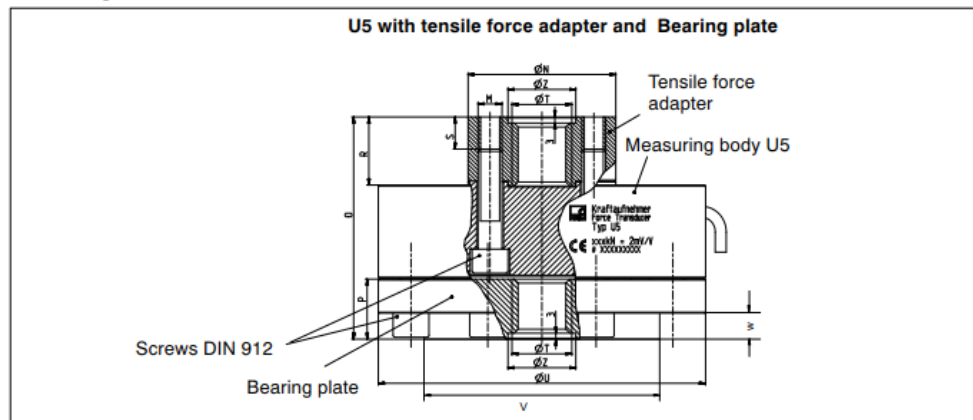


Space required for cable socket

wh (white)	Measurement signal (+) U_A	1	
bk (black)	Excitation voltage (-) U_B	2	
rd (red)	Measurement signal (-) U_A	4	
bu (blue)	Excitation voltage (+) U_B	3	
gn (green)	sensor circuit (+)	6	
gr (grey)	sensor circuit (-)	7	
Cable shielding, connected to housing		5 (no function)	

Pin assignment

Mounting accessories



Mounting accessory for measurement of tensile force (tensile force adapter)

Nominal force	∅ N	M	O	P	R	S	∅ T	∅ U	V	W	∅ Z ^{+0,1}	Weight bearing plate (kg)
100 kN	74	M12	111	30	34	approx. 16	M30x2	164	118	13	34	approx. 3.9
200 kN	96	M16	137	40	44	approx. 20	M39x2	190	136	17	43	approx. 6.5
500 kN	138	M20	224.5	80	81.5	approx. 55	M72x4	260	190	35	76	approx. 25

Adapter

100 kN:

Tensile force adapter each with 8 screws (M12 x 50)
Bearing plate each with 8 screws (M12 x 30)

Order no. 2-9278.0350
Order no. 2-9278.0351

200 kN:

Tensile force adapter each with 8 screws (M16 x 55)
Bearing plate each with 8 screws (M16 x 40)

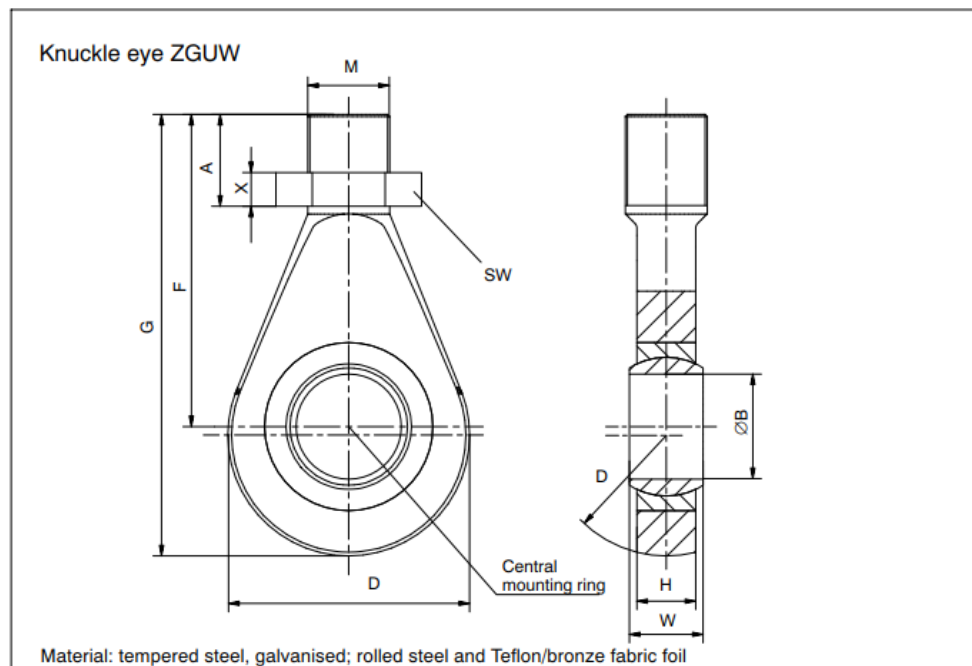
Order no. 2-9278.0353
Order no. 2-9278.0354

500 kN:

Tensile force adapter each with 8 screws (M20 x 65)
Bearing plate each with 8 screws (M20 x 65)

Order no. 2-9278.0356
Order no. 2-9278.0357

Mounting accessories (Dimensions in mm)



Nominal force kN	Order no. Knuckle eye ZGUW	Weight kg	A	ØB	D	F	G	H	M	SW	W	X
100	1-Z4/100kN/ZGUW	1.3	66.5	30 ^{H7}	70	110.5	145.5	25	M30x2	46	37	24
200	1-U2A/10t/ZGUW	1.1	65.5	50 ^{+0.002 -0.014}	115	148.5	210	28	M39x2	60	35	16
500	1-Z4/500kN/ZGUW	12.5	80	60 ^{+0.003 -0.018}	180	255	352	36	M72x4	-*)	44	

* secured with 2 screws to prevent rotation

Modifications reserved.
All details describe our products in general form only. They are not to be understood as express warranty and do not constitute any liability whatsoever.

B0793-4.3 en

Hottinger Baldwin Messtechnik GmbH

Im Tiefen See 45, D-64293 Darmstadt, Germany
Tel.: +49 6151 803-0 Fax: +49 6151 803 9100
Email: support@hbm.com Internet: www.hbm.com



measurement with confidence

Hiwin RGW45CC Linear Guideway Specifications [2].

RGW

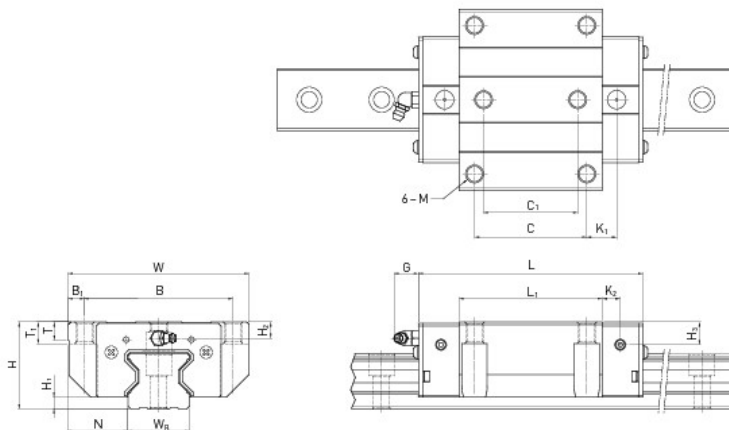


Table Dimensions of the block

Series/ size	Installation dimensions [mm]			Dimensions of the block [mm]													Load ratings [N]		Weight [kg]	CAD		
	H	H ₁	N	W	B	B ₁	C	C ₁	L ₁	L	K ₁	K ₂	G	M	T	T ₁	H ₂	H ₃			C _{dyn}	C ₀
RGW45CC	60	8,0	37,5	120	100	10	80	60	106,0	153,2	21,00	10,00	12,9	M12	14,0	15	10,0	14,0	92600	178800	3,43	CAD

Dimensions of the rail

Load ratings and torques

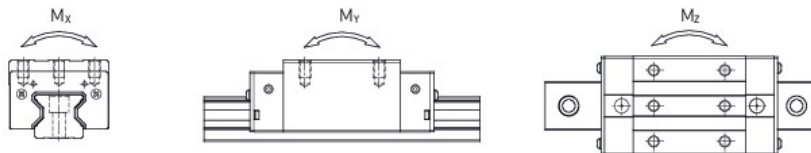


Table Load ratings and torques for series RG/QR

Series/size	Dynamic load rating C _{dyn} [N]*	Static load rating C ₀ [N]	Dynamic moment [Nm]			Static moment [Nm]		
			M _x	M _y	M _z	M _{0x}	M _{0y}	M _{0z}
RG_45C	92600	178800	2340	1579	1579	4520	3050	3050

* Dynamic load rating for travel distance of 100 000 m

Hiwin Linear Guideways Mounting Positions [3, p. 16–17].

Linear guideways

General information

2.7 Mounting position

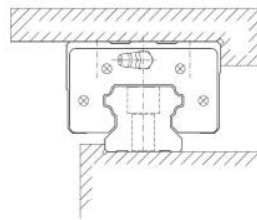
2.7.1 Examples of typical mounting positions

A linear guideway can absorb loads from above/below and right/left. The mounting position depends on the requirements of the machine and the loading direction. The precision of the rail is defined by the straightness and evenness of the installation surfaces, since the rail is attached to these while the screws are being tightened.

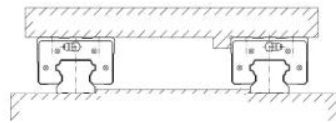
Profile rails that are not attached to an installation surface may have larger tolerances in terms of straightness. Below you will find typical mounting situations: Details of the assembly tolerances can be found in the chapters for the individual series.

A profile bar on a reference edge:

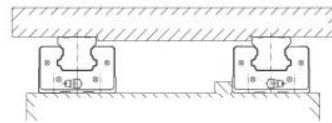
The reference edge is identified by arrows on the top of the rail. For very short rails, identification is on the front side of the rail.



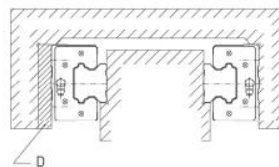
Two rails with mobile block:



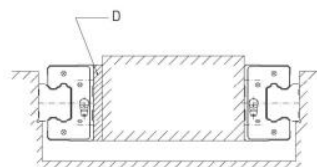
Two rails with permanently installed block:



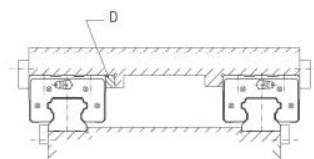
Two external blocks:



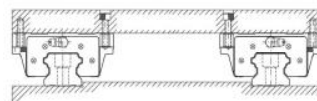
Two internal blocks:



Setup with permanently installed surface:



HGW..C block with different mounting directions:



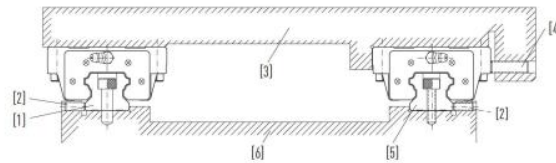
D Spacer

2.8 Assembly

Depending on the accuracy required and the linear guideway's impact and vibration loading, the following three types of assembly are recommended.

2.8.1 Assembly of rails with reference edge and clamp

If the machine is subject to severe vibration, impact or lateral force, guides and blocks may move. To avoid this problem and achieve a high level of rigidity and guidance accuracy, we would recommend assembling the linear guideway with reference edges and clamps on both sides.

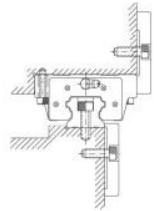


- [1] Following side
- [2] Guide clamping screw
- [3] Carriage
- [4] Block clamping screw
- [5] Reference side
- [6] Machine bed

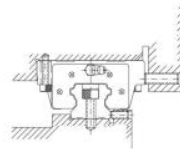
2.8.1.1 Types of attachment

The following four types of attachment are recommended

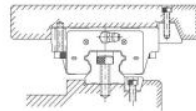
Attachment with a clamping plate:



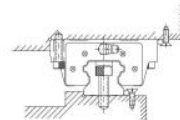
Attachment with clamping screws:



Attachment with clamping strips:



Attachment with needle rollers:



The Dowel Pin Calculations

Without pins and 8.8 screws																
Bolt	Connector	Shear Force N	Axial Force N	Bending moment Nm	t Mpa	tsall Mpa	FoS	σ Mpa	osall Mpa	FoS	σt Mpa	osall Mpa	FoS	σvert Mpa	osall Mpa	FoS
1	Counterbore Screw-78	2986,7	40800	43,9	35,4	369,5	10,4	484,0	640,0	1,3	201,2	640,0	3,2	643,3	640,0	1,0
2	Counterbore Screw-79	3190	40345	46,5	37,8	369,5	9,8	478,6	640,0	1,3	213,2	640,0	3,0	650,8	640,0	1,0
3	Counterbore Screw-80	3088,3	40550	46,7	36,6	369,5	10,1	481,0	640,0	1,3	213,8	640,0	3,0	653,5	640,0	1,0
4	Counterbore Screw-81	2303,9	39715	34,1	27,3	369,5	13,5	471,1	640,0	1,4	156,4	640,0	4,1	587,6	640,0	1,1
5	Counterbore Screw-82	2427	39610	35,0	28,8	369,5	12,8	469,9	640,0	1,4	160,6	640,0	4,0	590,4	640,0	1,1
6	Counterbore Screw-83	1027,7	3923	11,9	12,2	369,5	30,3	46,5	640,0	13,8	54,4	640,0	11,8	103,7	640,0	6,2
With pins and 12.9 screws																
Bolt	Connector	Shear Force N	Axial Force N	Bending moment Nm	t Mpa	tsall Mpa	FoS	σ Mpa	osall Mpa	FoS	σt Mpa	osall Mpa	FoS	σvert Mpa	osall Mpa	FoS
1	Counterbore Screw-78		40800	43,9	0,0	635,1		484,0	1100,0	2,3	201,2	1100,0	5,5	642,4	1100,0	1,7
2	Counterbore Screw-79		40345	46,5	0,0	635,1		478,6	1100,0	2,3	213,2	1100,0	5,2	649,7	1100,0	1,7
3	Counterbore Screw-80		40550	46,7	0,0	635,1		481,0	1100,0	2,3	213,8	1100,0	5,1	652,4	1100,0	1,7
4	Counterbore Screw-81		39715	34,1	0,0	635,1		471,1	1100,0	2,3	156,4	1100,0	7,0	587,0	1100,0	1,9
5	Counterbore Screw-82		39610	35,0	0,0	635,1		469,9	1100,0	2,3	160,6	1100,0	6,9	589,7	1100,0	1,9
6	Counterbore Screw-83		3923	11,9	0,0	635,1		46,5	1100,0	23,6	54,4	1100,0	20,2	103,0	1100,0	10,7
Overall shear force		15023,6 N														
Mean bending moment		39,5 Nm														
Number of Pins		2														
Strength of the pin																
Allowable Shear		635,1 Mpa														
Allowable bending		1100 MPa														
Required diameter (min)		5,81 mm														
Shear stress		283,34 Mpa														
bending stress		1 025,08 MPa														
Von Mises stress		1100,61 MPa														

Connector: Counterbore Screw-78 Units: SI

Connector type: Bolt

Type	X-Component	Y-Component	Z-Component	Resultant
Shear Force (N)	-108,62	0	-2984,7	2986,7
Axial Force (N)	0	0	40800	40800
Bending moment (N.m)	43,887	0	-1,4003	43,91

Study name: 4000450-LC9-45501

Connector: Counterbore Screw-81 Units: SI

Connector type: Bolt

Type	X-Component	Y-Component	Z-Component	Resultant
Shear Force (N)	-1445,5	0	-1794	2303,9
Axial Force (N)	0	0	39715	39715
Bending moment (N.m)	23,998	0	-24,265	34,127

Study name: 4000450-LC9-45501

Connector: Counterbore Screw-79 Units: SI

Connector type: Bolt

Type	X-Component	Y-Component	Z-Component	Resultant
Shear Force (N)	448,9	0	-3158,2	3190
Axial Force (N)	0	0	40345	40345
Bending moment (N.m)	45,891	0	7,6863	46,531

Study name: 4000450-LC9-45501

Connector: Counterbore Screw-82 Units: SI

Connector type: Bolt

Type	X-Component	Y-Component	Z-Component	Resultant
Shear Force (N)	1393,1	0	-1987,4	2427
Axial Force (N)	0	0	39610	39610
Bending moment (N.m)	25,897	0	23,603	35,039

Study name: 4000450-LC9-45501

Connector: Counterbore Screw-80 Units: SI

Connector type: Bolt

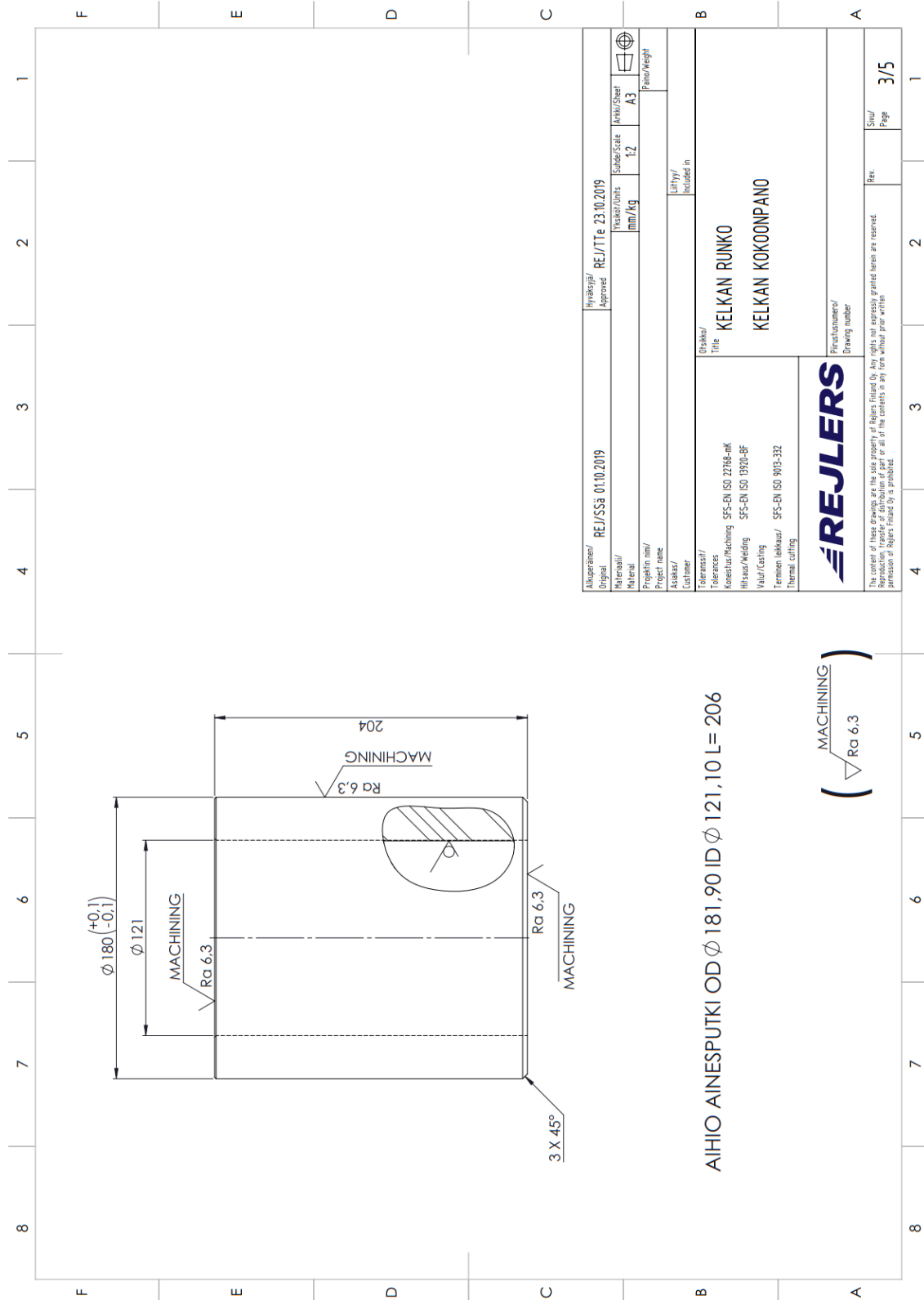
Type	X-Component	Y-Component	Z-Component	Resultant
Shear Force (N)	-471,36	0	-3052,1	3088,3
Axial Force (N)	0	0	40550	40550
Bending moment (N.m)	46,107	0	-7,1499	46,658

Study name: 4000450-LC9-45501

Connector: Counterbore Screw-83 Units: SI

Connector type: Bolt

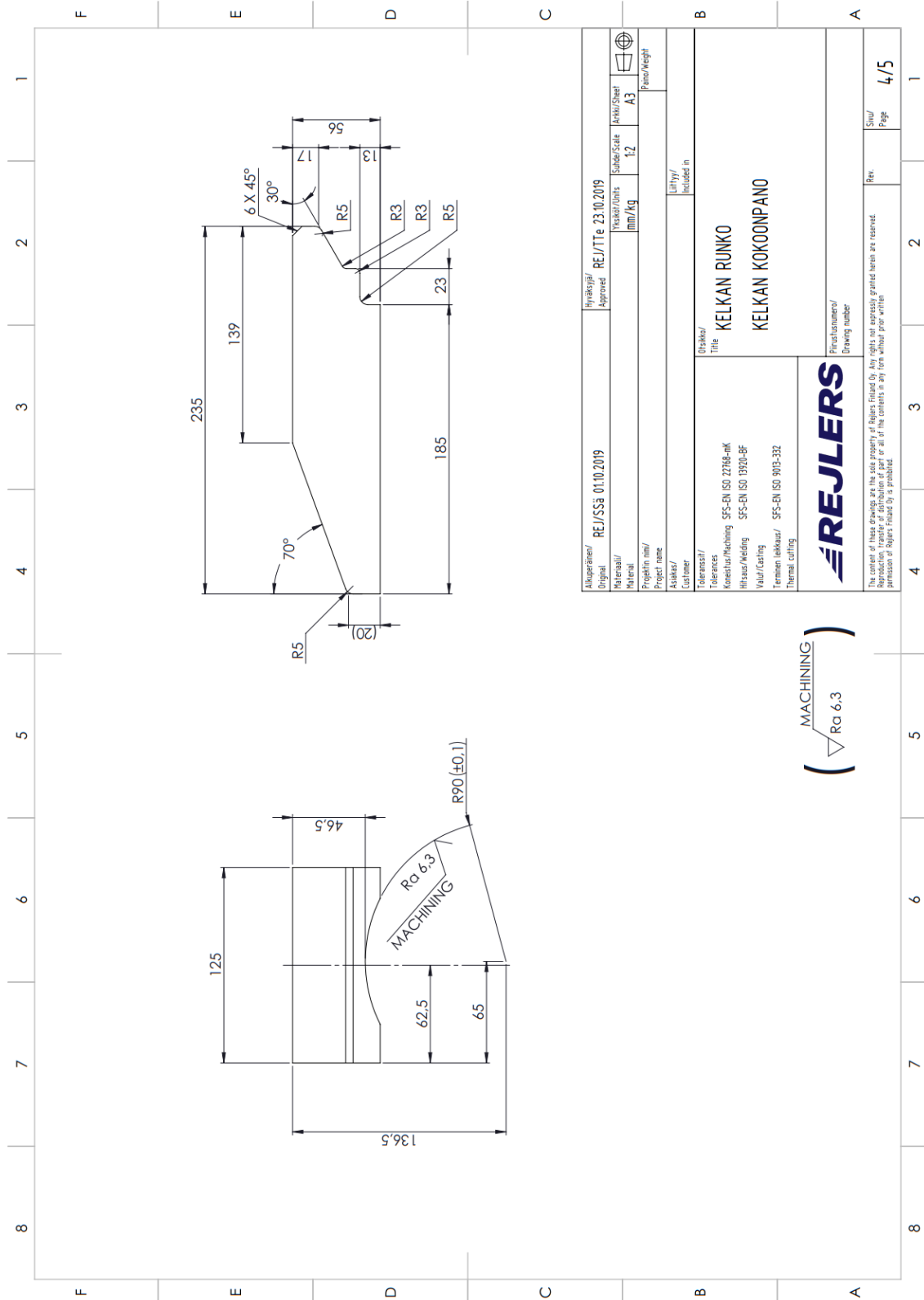
Type	X-Component	Y-Component	Z-Component	Resultant
Shear Force (N)	-128,33	0	-1019,7	1027,7
Axial Force (N)	0	0	39623	39623
Bending moment (N.m)	11,567	0	-2,6441	11,565



AIHIO AINESPUTKI OD $\varnothing 181,90$ ID $\varnothing 121,10$ L= 206

(MACHINING)
Ra 6.3

Aluepiirite/ Original	REJ/SS3 01.10.2019	Hyväksyjä/ Approved	REJ/TTe 23.10.2019	Subo-Scale	1:2	Lehti/Sheet	A3	
Materiaali/ Material		Tekijä/Units		mm/Kg		Page/Weight		
Projektin nimi/ Project name		Asiakas/ Customer		Lähtö/ Included in				
Toleranssi/ Tolerances		Ohjeet/ Title	KELKAN RUNKO					
Koneistus/Machining	SFS-EN ISO 22768-mK		KELKAN KOKOONPANO					
Hitaus/Welding	SFS-EN ISO 13920-BF							
Valu/Casting	SFS-EN ISO 9003-332							
Termoin leikkaus/ Thermal cutting								
REJLERS				Pääpiirite/ Drawing number				
The content of these drawings are the sole property of Rejlers Finland Oy. Any rights not expressly granted herein are reserved. Reproduction, transfer of distribution of part or all of the contents in any form without prior written permission of Rejlers Finland Oy is prohibited.							Rev.	3/5



Alkuperäinen / Original	REJ/SSä 01.10.2019	Hyväksyjä / Approved	REJ/TTe 23.10.2019	Leikkurimäärä / Pieces	12	Leikkurivälit / Sheet	A3	Paino / Weight	
Materiaali / Material		Projekti nimi / Project name		Leikkurimäärä / Pieces		Leikkurivälit / Sheet			
Asiakas / Customer		Asiakas / Customer		Leikkurimäärä / Pieces		Leikkurivälit / Sheet			
Toleranssi / Tolerances		Asiakas / Customer		Leikkurimäärä / Pieces		Leikkurivälit / Sheet			
Koneistus / Machining	SFS-EN ISO 22768-mik	Asiakas / Customer		Leikkurimäärä / Pieces		Leikkurivälit / Sheet			
Hitaus / Welding	SFS-EN ISO 13920-BF	Asiakas / Customer		Leikkurimäärä / Pieces		Leikkurivälit / Sheet			
Valu / Casting		Asiakas / Customer		Leikkurimäärä / Pieces		Leikkurivälit / Sheet			
Termen leikkaus / Thermal cutting	SFS-EN ISO 9013-332	Asiakas / Customer		Leikkurimäärä / Pieces		Leikkurivälit / Sheet			
		Otsikko / Title KELKAN RUNKO KELKAN KOKOONPANO		LIIHTY / Included in					
		Piirustuksen / Drawing number		Rev. / Page 4/5					

(MACHINING)
 (Ra 6.3)

